Quaternary Science Advances 3 (2021) 100019

Contents lists available at ScienceDirect

Quaternary Science Advances

journal homepage: www.journals.elsevier.com/quaternary-science-advances

Climate and ocean forcing of ice-sheet dynamics along the Svalbard-Barents Sea ice sheet during the deglaciation ~20,000–10,000 years BP

Tine L. Rasmussen [a,*], Erik Thomsen [b]

[a] CAGE, Centre for Arctic Gas Hydrate, Environment and Climate, Department of Geosciences, UiT the Arctic University of Norway, Tromsø, Norway
[b] Department of Geoscience, Aarhus University, Aarhus, Denmark

ARTICLE INFO

Keywords:
Ice retreat rates
Storfjorden ice stream
Paleoceanography
Paleoclimate
Paleotemperature

ABSTRACT

The last deglaciation, 20,000–10,000 years ago, was a period of global warming and rapidly shrinking ice sheets. It was also climatically unstable and retreats were interrupted by re-advances. Retreat rates and timing relative to climatic changes have therefore been difficult to establish. We here study a suite of 12 marine sediment cores from Storfjorden and Storfjorden Trough, Svalbard. The purpose is to reconstruct retreat patterns and retreat rates of a high northern latitude marine-based ice stream from the Svalbard-Barents Sea Ice Sheet in relation to paleoceanographic and paleoclimatic changes. The study is based on abundance and composition of planktic and benthic foraminiferal assemblages, ice rafted debris (IRD), lithology, and 70 AMS-^{14}C dates. For core 460, we also calculate sea surface and bottom water temperatures and bottom water salinity. The results show that retreat rates of the ice shelf and ice streams of Storfjorden Trough/Storfjorden ('Storfjorden Ice Stream') closely followed the deglacial atmospheric and ocean temperature changes. During the start of the Bølling interstadial retreat rates in Storfjorden Trough probably exceeded 2.5 km/year and more than 10,000 km^2 of ice disappeared almost instantaneously. A similarly rapid retreat occurred at the start of the Holocene interglacial, when 4500 km^2 of ice broke up. Maximum rates during the deglaciation match the fastest modern rates from Antarctica and Greenland. Correlation of data show that the ice streams in several fjords from northern Norway retreated simultaneously with the Storfjorden Ice Stream, indicating that temperature was the most important forcing factor of the Svalbard-Barents Sea Ice Sheet during the deglaciation.

1. Introduction

The majority of the World's marine ice sheets are thinning and retreating rapidly (Howat et al., 2010; Rignot et al., 2013, 2019; Konrad et al., 2018). In Greenland, Jacobshavn Isbræ to the west and Helheim and Kangerlussuaq glaciers to the east have retreated up to 4 km in two years (Luckman et al., 2006). Similar rates have been obtained from both East and West Antarctica. In the Amundsen Sea, west Antarctica, the grounding line (the line where grounded ice becomes afloat) of the Pine Island Glacier retreated with a rate of 1–2 km/year between 1992 and 2011 (Park et al., 2013; Rignot et al., 2014). The grounding lines of the Smith and Pope glaciers show retreat rates of 2 km/year and 0.5 km/year, respectively, from 1996 to 2016 (Scheugl et al., 2016). For many of these glaciers, the retraction is due to basal melting from intrusion of warm subsurface water alongside with the atmospheric heating, both related to the ongoing global climate warming (Luckman et al., 2006; Cook and Vaughan, 2010; Holland et al., 2008; Howat et al., 2010; Murray et al., 2010; Jacobs et al., 2011; Hughes et al., 2012; Bjørk et al., 2012; Mouginot et al., 2015; Rintoul et al., 2016; Hogg and Gudmundsson, 2017; Hogg et al., 2017; Konrad et al., 2018; Rignot et al., 2019). Local advances have also been recorded, but they are relatively few compared to retreats.

In the northern Hemisphere, the deglaciation was characterized by three major rapid warming phases, the Bølling and Allerød interstadials and the Holocene interglacial, interrupted by three periods of cooling, of which the Younger Dryas stadial was the most severe (Johnsen et al., 1992). The Older Dryas is a short-lasting cold event separating the Bølling and Allerød interstadials (e.g., Björck et al., 1996). The warmings at the beginning of the Bølling interstadial and Holocene interglacial were particularly strong and fast with temperature increases in Greenland of up to 12–16 °C within a few decades (Johnsen et al., 2001; Steffensen et al., 2008). Earlier work indicate that the deglaciation of the continental margin of Svalbard follows the anticipated pattern with maximum retreat during the major warm phases and with halts or

* Corresponding author.
E-mail address: tine.rasmussen@uit.no (T.L. Rasmussen).

https://doi.org/10.1016/j.qsa.2020.100019
Received 25 May 2020; Received in revised form 12 October 2020; Accepted 6 November 2020
Available online 11 November 2020

re-advances during the cold intervals (Svendsen et al., 1996; Landvik et al., 2005; Hogan et al., 2017; Nielsen and Rasmussen, 2018). However, previous studies are few and no attempts have been made to quantify rates of retreat.

In contrast to Svalbard, several studies with quantitative estimates of retreat rates are available from the southern Barents Sea Ice Sheet, the Fennoscandian and British Ice Sheets (e.g., Vorren and Plassen, 2002; Junttila et al., 2010; Stokes et al., 2014; Åkesson et al., 2018; Small et al., 2018; Ó Cofaigh et al., 2019; Brendryen et al., 2020; Bradwell et al., 2019, 2020). However, the conclusions of some of these studies are often disparate to the modern studies as they find that changes in retreat rates were uncorrelated to climatic changes. Instead, they invoke surface geometry, e.g., topographic lows and highs, fjord width, substrate and water depth, as the primary controlling factor (e.g., Briner et al., 2009; Stokes et al., 2014; Small et al., 2018; Bradwell et al., 2019; Lowry et al., 2020), thus, Stokes et al. (2014) concluded that the fastest retreats of eight glaciers in northern Norway generally occurred independent of the atmospheric warmings and, furthermore, were asynchronous between individual glaciers.

Here we study the deglaciation history of the Storfjorden Trough/Storfjorden from the northwestern part of the Svalbard-Barents Sea Ice Sheet from the end of the Last Glacial Maximum to the early Holocene (20,000 to ~10,000 years ago). The investigation is based on a suite of marine cores from close to the shelf edge to the innermost part of the fjord. The chronostratigraphy of the study is supported by 70 AMS-^{14}C dates. The climatic and oceanographic reconstructions include sea surface and bottom water temperatures and bottom water salinity calculated from distributional data of planktic and benthic foraminiferal faunas. The dataset also comprises several lithological parameters including the distribution of laminated deposits and the occurrence of ice rafted debris (IRD).

The study is based on marine cores taken in/or in front of former ice-stream grounding zones (Fig. 1). For studies of ice retreat, such records seem to offer several advantages. Firstly, the presence of micro- and macrofossils ensures that most marine records can be dated by the AMS-^{14}C method, which is a relative precise dating tool although

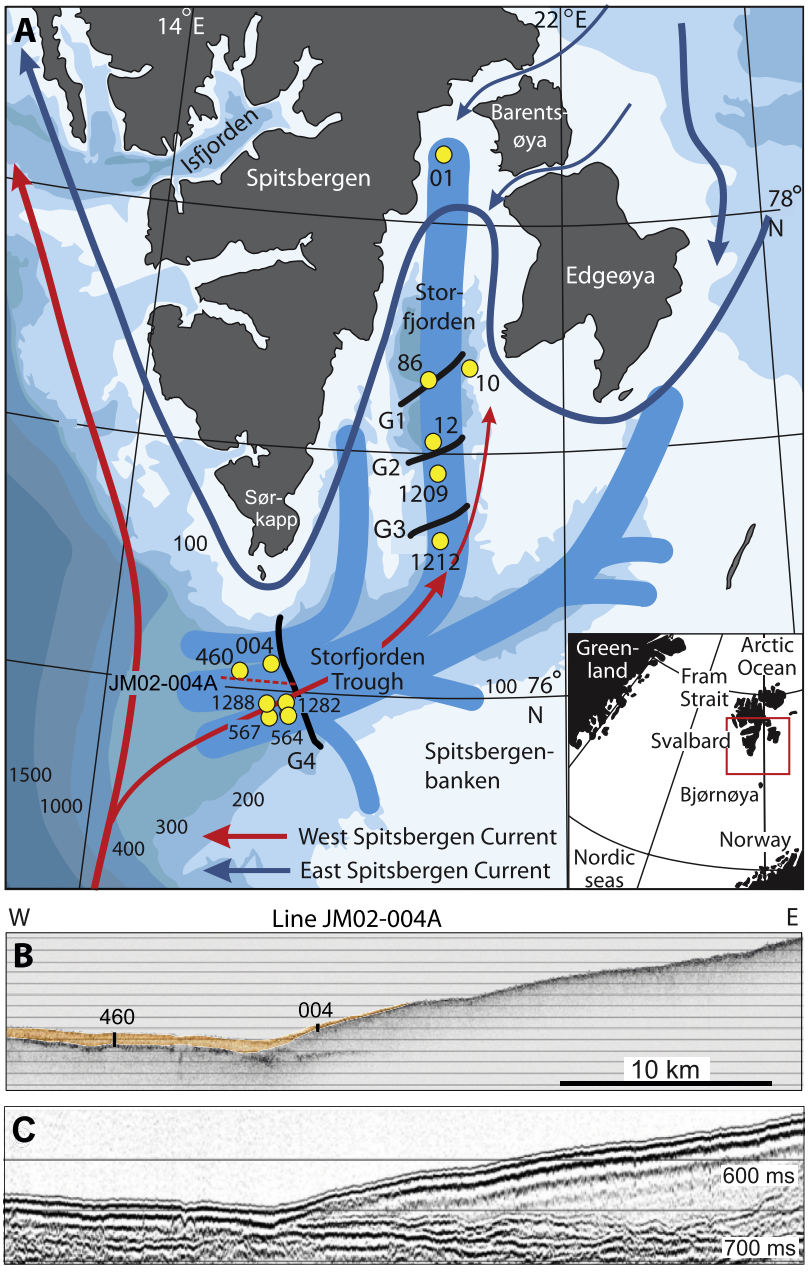

Fig. 1. Map of Storfjorden Trough and Storfjorden with major cold and warm ocean currents, core locations and ice-streams here collectively termed 'Storfjorden Ice Stream'. (a) Insert map shows the northern Nordic Seas and the location of the Svalbard archipelago. Black lines indicate grounding lines of the respective grounding zones G1–G4, with G1–G3 described by Nielsen and Rasmussen (2018) and termed inner, middle and outer grounding zones, respectively. Courses of ice-streams are based on Nielsen and Rasmussen (2018) and Pedrosa et al. (2011). Base map is modified from Rasmussen and Thomsen (2014), (b) West-east 'chirp'-profile JM02-004 (3.5 kHz deep-penetrating echo-sounding) based on a 2002 crossing of grounding zone G4. The profile shows western part of G4 with location of core 460 marked. The top sediment package (marked with a brownish colour) is ~6 m thick and consist of glacial, deglacial and Holocene deposits. This layer thins eastward over G4, where it consists of deglacial sediments with a thin Holocene lag deposit on top. Core 004, taken slightly north of the line, is projected onto the profile, (c) Seismic profile line JM02-004 LegA (same trajectory as 'chirp' line in (b)). The profile indicates the overall seismic structure of G4. Panels B and C, courtesy of A. Solheim, Norwegian Geotechnical Institute, Oslo, Norway.

unknown changes in reservoir ages can sometimes hamper correlations. Secondly, marine cores taken near ice fronts often contain alternating glacimarine (tills/diamictons) and hemipelagic deposits providing straightforward and datable evidence of ice movements. Thirdly and most importantly, marine records generally carry their own paleoclimate and -environmental records (micro- and macrofossils, IRD, etc.) often reflecting changes in both the local and the regional/global climate history (e.g., Svendsen et al., 1996; Landvik et al., 2005; Scourse et al., 2009; Junttila et al., 2010; Hogan et al., 2017; Laberg et al., 2018; Ó Cofaigh et al., 2019; Bradwell et al., 2020).

The overall purpose of the study is threefold: 1) to analyse retreats and advances of the Storfjorden Trough/Storfjorden ice streams relative to the rapid changes in atmospheric and oceanic temperatures and fast increase in sea level that characterized the deglaciation, 2) compare the results from Storfjorden Trough/Storfjorden with studies from the northern Fennoscandian Ice Sheet for regional comparison and correlation of ice retreat dynamics, and 3) compare the reconstructed retreat rates from high-latitude Svalbard with modern retreat rates.

1.1. Geological and oceanographical setting

During the last glaciation, the Storfjorden Trough ice streams constituted a substantial segment of the western border of the Svalbard-Barents Sea Ice Sheet terminating toward the northernmost Atlantic (Laberg and Vorren, 1996). The ice-stream occupying Storfjorden Trough was a merger of three separate ice-streams (Pedrosa et al., 2011) with the ice stream from Storfjorden forming the central part (Nielsen and Rasmussen, 2018) (Fig. 1A), hereafter collectively referred to as 'Storfjorden Ice Stream'. Four transverse ridges are interpreted as ice grounding zones marking the position of former ice grounding lines (Grounding zones G1–G4) (Fig. 1). Grounding zones G1–G3 are located in Storfjorden. They have previously been named 'inner, middle and outer' grounding zones and dated to 11,700, 14,500 and 15,300 years, respectively (Nielsen and Rasmussen, 2018). The fourth grounding zone (G4) is situated in outer Storfjorden Trough about 50 km from the shelf edge and was surveyed in 2002 (Fig. 1B and C). A geomorphologic study of this grounding zone was published by Shackleton et al. (2020).

Today, the area is affected by a branch of the West Spitsbergen

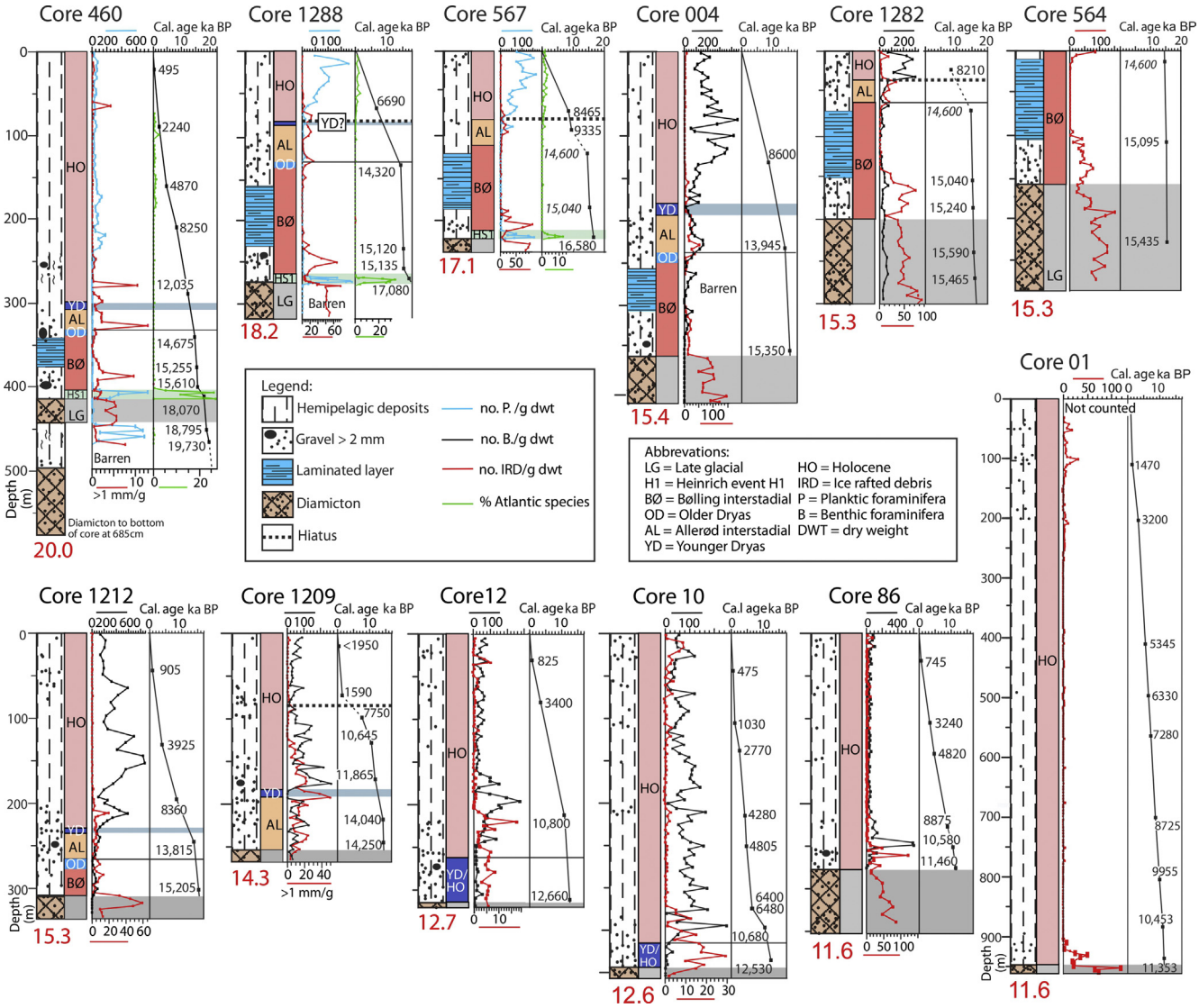

Fig. 2. Lithology, stratigraphy, calibrated AMS-^{14}C dates and age models for the investigated cores. For each core, we also show concentrations of foraminiferal faunas, ice rafted debris (IRD) (in number/g dry weight sediment) and percentages of subtropical to boreal benthic species ('Atlantic species') (see list in Fig. 3). Basal diamictons/coarse glacimarine sediments are indicated by light brownish colour. A distinctive laminated clay assigned to the Bølling Interstadial is marked by a bluish colour. Numbers in red below each lithological column gives the estimated age (in ka) of the oldest marine deposits in that particular core. Older Dryas (OD) and Younger Dryas (YD) are defined by high relative abundance of agglutinated foraminifera as shown for cores 460 and 1209 in Rasmussen and Thomsen (2014).

Current carrying warm Atlantic surface water derived from the Norwegian-Atlantic Current into Storfjorden Trough and to the eastern part of Storfjorden (Fig. 1). Cold Arctic surface water of the East Spitsbergen Current coming from the Arctic Ocean flows along the coastline continuing northward on the inner shelf of Spitsbergen (e.g., Loeng, 1991).

2. Material and methods

The study is based on 12 sediment cores taken from outer Storfjorden Trough and into Storfjorden covering a distance of ~350 km (Figs. 1 and 2; Table 1). Six of the cores were described in Rasmussen et al. (2007), Rasmussen and Thomsen (2014), and Nielsen and Rasmussen (2018). The six new cores target the hitherto un-dated grounding zone G4 and the innermost part of Storfjorden as close to land as possible (Fig. 1). The new cores add long distance information not previously available and are crucial for the calculation of retreat rates.

The 12 cores were taken between 2002 and 2016 in Storfjorden and Storfjorden Trough (Figs. 1 and 2). Two of the new cores, 1288 and 567, were taken in front of grounding zone G4, while cores 004, 1282 and 564 were retrieved within G4 (Figs. 1 and 2; Table 1). These five cores were taken from 2014 to 2016 on cruises with RV *Helmer Hanssen*, UiT the Arctic University of Norway. Kullenberg core 01, from the northernmost part of Storfjorden, was retrieved in 2016 during a cruise with the French Research Vessel *l'Atalante*, IFREMER (Michel et al., 2016).

The six new cores were cut into 1-cm slices. Samples were weighed, freeze-dried, and weighed again, before wet sieved over 0.063, 0.1 and 0.5 mm sieves. Ice rafted debris (IRD) was counted in the size-fraction >0.5 mm except for cores 1209 (Rasmussen and Thomsen, 2014) and 460 (Rasmussen et al., 2007) that were counted in the >1 mm size fraction. More than 300 specimens each of benthic and planktic foraminifera were counted in the >0.1 mm fraction. Percentages of benthic foraminiferal species of subtropical-boreal affinity were added together and referred to as the 'Atlantic species group' (see e.g., Rasmussen et al., 1996; 2007). They comprise species of *Gyroidina*, *Epistominella*, *Cibicidoides*, *Pullenia* and several miliolid species (see list in Fig. 3). Today, these species are most common at water temperatures above 2–3.5 °C (see references in Rasmussen and Thomsen, 2004). Concentrations of IRD, benthic and planktic foraminifera were calculated as number per gram dry weight sediment (Fig. 2). Oxygen isotope ratios ($\delta^{18}O$) were previously published in Rasmussen et al. (2007). The values were measured on the planktic foraminiferal species *Neogloboquadrina pachyderma* s and the benthic species *Melonis barleeanus*, *Cibicides lobatulus*, and *Elphidium excavatum* (Fig. 3) (see Rasmussen et al., 2007 for details of methods).

Samples of mollusks and/or foraminifera were dated by AMS-^{14}C datings at 14Chrono Centre, Queen's University, Belfast, Northern Ireland or at the AMS-^{14}C Dating Centre, Aarhus University, Denmark (Table 2). All dates were calibrated using the Calib7.04, Marine13 program (Reimer et al., 2013). The age of the mid-point of 1-sigma error was chosen (Table 2). A standard reservoir age of −405 years inherent in the calibration program was used. Ages are presented in calendar years before present (=AD 1950 CE). The same procedure was followed as for the previously published cores from Storfjorden (Nielsen and Rasmussen, 2018; Rasmussen and Thomsen, 2014), while the dates of core 460 were re-calibrated for this study.

Surface and bottom water temperatures and salinities for core 460 were estimated by transfer functions using the C2 program (Juggins, 2007) (Fig. 3). For comparison, we also calculated bottom water temperatures for cores 1288 and 567. We used the same procedures and databases as outlined in Rasmussen et al. (2014). We applied the WAPLS (Weighed Average Partial Least-Squares) method using two components. Surface water temperatures were calculated based on the >150-μm size fraction of planktic foraminifera using the MARGO database (Kucera et al., 2005) together with sea surface temperatures from the World Ocean Atlas 2009 (Locarnini et al., 2010). For calculating bottom water temperature and salinity, we used the same database of Sejrup et al. (2004) with the same modifications as outlined in Rasmussen et al. (2014). The mean standard error of prediction for core 460 is 1.44 for the benthic temperatures and 1.93 for the planktic temperatures (Fig. 3). The values are primarily the result of the size of the training set. The larger planktic database (training set) produces higher error values than the smaller benthic database.

Table 1
Positions and water depth of the investigated cores.

Core Name	Latitude	Longitude	Water depth (m)
JM02-460 PC	76.055197°	15.987881°	389
HH15-1288 GC	75.842517°	16.584083°	358
HH16-567 GC	75.842567°	16.583567°	356
HH14- 004 GC	76.024917°	16.191350°	377
HH15-1282 GC	75.839533°	16.631167°	349
HH16-564 GC	75.839500°	16.631400°	346
HH12-1212 GC	76.616850°	19.548433°	178
HH12-1209 GC	76.902967°	19.434467°	151
JM10-12 GC	77.122633°	19.407650°	146
JM10-10 GC	77.385049°	20.031091°	123
NP05-86 GC	77.360000°	19.307667°	141
STEP16-K01	78.249951°	19.499596°	109

3. Results

All cores reach into coarse, unsorted sediments with gravel and sand in a silt-clay matrix interpreted as tills/diamictons (generally barren of micro- and macrofauna) or very coarse glacimarine sediments (in cores 1282, 564, 1212, 10 and 12 a diverse micro- and macrofauna may be present in certain horizons) (Fig. 2). The age of the earliest marine deposits in all cores was estimated by AMS-^{14}C datings of the oldest normal glacimarine/hemipelagic sediments taken as close to the tills/diamictons as possible (Fig. 2). The age model of core 460 from the outer trough closest to the shelf edge has been published previously (Rasmussen et al., 2007) (Figs. 2 and 3 4). This core contains a complete high-resolution, undisturbed stratigraphical record with no apparent hiati in the section relevant for this study and it can therefore serve as a reference for the stratigraphy of the Storfjorden Trough/Storfjorden area. The record of core 460 comprises the time period~ 20,000 years to present and comprises the time intervals late LGM (~20,000–19,000 years), Heinrich stadial HS1 (19,000–15,600 years) (time equivalent to North Atlantic Heinrich event H1 (e.g., Bond et al., 1993)), the well-known Bølling and Allerød interstadials (15,600–13,000 years), the Younger Dryas stadial (13,000–11,700 years) and the Holocene (11,700–0 years) (see Rasmussen et al., 2007) (Fig. 2).

3.1. Age models and event stratigraphy

All dates are calibrated AMS-^{14}C dates (see above; Table 2). Age models for the three cores from the outer part of Storfjorden Trough with the longest records were calculated assuming linear sedimentation between dating points. Dating errors are largest in core 460 analyzed in 2002 (Rasmussen et al., 2007). The later dates have small errors with a maximum of 165 years. For cores 567, 1282 and 564, we used previously obtained ages for a distinct laminated horizon as fix points (marked in italics in Fig. 2); otherwise all age models are independent with no attempts of synchronisation (see below). We observe a single age reversal in the lower part of the diamicton of core 564 (Table 2). The reversal is most likely due to downward transport of a younger shell during the coring process (Fig. 2).

The lower boundaries of the Bølling and Allerød Interstadials, the Younger Dryas stadial and the Holocene interglacial constitute the chronostratigraphical framework for this study. Numerous studies have demonstrated that each of the four boundaries or events are easily distinguished by a characteristic and distinct set of lithological and faunistic shifts that makes them identifiable all over the Nordic Seas and

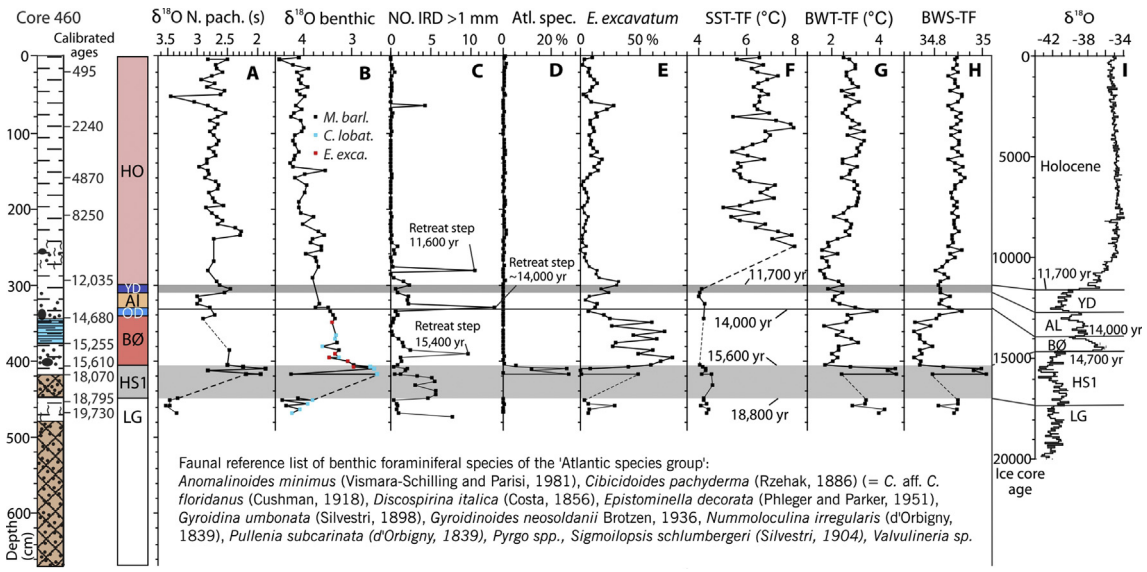

Fig. 3. Lithology, stratigraphy and selected data from reference core 460 from outer Storfjorden Trough compared to Greenland ice core NGRIP: (a) Oxygen isotope record measured on planktic foraminiferal species *Neogloboquadrina pachyderma* s, (b) Composite oxygen isotope record measured on benthic foraminiferal species *Melonis barleeanus* (black squares), *Cibicides lobatulus* (blue squares) and *Elphidium excavatum* (red squares), (c) Concentration of ice rafted debris (IRD) given as number of mineral grains >1 mm per gram dry weight sediment, (d) Percentage of subtropical-boreal benthic foraminiferal species (termed 'Atlantic species') (species listed with references in lower part of figure), (e) Percentage of polar benthic foraminiferal species *Elphidium excavatum*, (f) Sea surface temperature (SST) and (g) bottom water temperature calculated by transfer functions performed on the planktic and benthic foraminiferal census data, (h) Bottom water salinity calculated by transfer functions performed on benthic foraminiferal census data, (i) Oxygen isotope record from NGRIP ice core plotted versus GICC05 age scale (data from Rasmussen et al., 2014). a–e, data from (Rasmussen and Thomsen, 2014), f–h, this study (see methods for details). Abbreviations and legend as in Fig. 2.

Barents Sea (see below, Figs. 2–4) (e.g., Elverhøi et al., 1995; Lubinski et al., 2001; Vorren and Plassen, 2002; Birgel and Hass, 2004; Ślubowska-Woldengen et al., 2007; Rasmussen et al., 2007; Junttila et al., 2010; Aagaard-Sørensen et al., 2010; Chistyakova et al., 2010; Jessen et al., 2010; Falardeau et al., 2018; Ivanova et al., 2019). The four boundaries are also extremely well dated and in cores retrieved from the Atlantic Water realm in the North Atlantic Ocean, the Nordic Seas and Barents Sea, they always obtain very similar dates (e.g., Duplessy et al., 1986, Elliot et al., 1998; Voelker et al., 1998; Waelbroeck et al., 2001, 2019; Nørgaard-Pedersen et al., 2003; Birgel and Hass, 2004; Bondevik et al., 2006; Stanford et al., 2011; Falardeau et al., 2018 and references therein).

However, correlation to the precise ages from annual layer counts in the Greenland ice cores (Rasmussen et al., 2014) demonstrates that the ^{14}C dates of the lower boundaries of the Bølling interstadial and the Younger Dryas stadial generally are too old when applying the standard reservoir age of around −400 years (Waelbroeck et al., 2001, 2019; Bondevik et al., 2006) (Fig. 3). This is exemplified by the start of the Bølling interstadial, which dates to 14,700 years in the Greenland ice core chronology (Rasmussen et al., 2014), but to 15,600 calendar years in records from the Nordic Seas and Barents Sea when using the standard correction (=~13,400 uncorrected ^{14}C years) (Vorren and Plassen, 2002; Nørgaard-Pedersen et al., 2003; Birgel and Hass, 2004; Jessen et al., 2010) (Fig. 3; Table 2). The start of the Allerød interstadial is an exception to this tendency as it dates to 14,000 years in the ice core (Rasmussen et al., 2014) and close to ~14,000 calendar years in the Nordic Seas (=~12,500 uncorrected ^{14}C years) (Svendsen et al., 1996; Vorren and Plassen, 2002; Nørgaard-Pedersen et al., 2003; Birgel and Hass, 2004; Bondevik et al., 2006; Jessen et al., 2010) (Fig. 2; Table 2). Overall, it is apparent that the reservoir ages of the Nordic Seas and Barents Sea during the deglaciation period generally were higher than the standard reservoir age, and, furthermore, could vary through time (Waelbroeck et al., 2001; Bondevik et al., 2006). It is, on the other hand, evident that the four events date very similarly in the Atlantic water zone of the Nordic Seas and Barents Sea indicating that within this water mass the variability is primarily temporal with only small spatial differences.

As all datings in this study are based on marine material, we prefer to use the marine ages and the marine identification of the interstadial-stadial boundaries (Figs. 2–5). We avoid further reservoir age corrections beyond the standard reservoir age of −405 years, as these are largely unknown for this region. The changes in reservoir age should not negatively affect the correlation between cores provided the dated materials are within the realm of Atlantic water, where these changes are synchronous or near synchronous (see above). This ensures us that the between-core correlations are reliable also on a regional scale from the Svalbard margin to the northern Norwegian margin (Fig. 1) (see below).

Furthermore, numerous studies have shown that the Bølling, Allerød and Holocene warmings in the Nordic Seas and Barents Sea, regardless of differences in reservoir age, correlate closely in time with the corresponding Bølling, Allerød and Holocene atmospheric warmings in the Greenland ice cores (Fig. 3). Some of these studies include several marine-ice core correlations based on solid tie-points such as tephra marker horizons (Davies et al., 2008, 2010; Voelker and Haflidason, 2015).

3.2. Bottom water temperatures

In Fig. 3, we show surface and bottom water temperatures for core 460 as estimated by transfer functions. The bottom water temperatures of 460 are compared to the bottom water temperatures of the nearby cores 1288 and 567 in Fig. 5, where we also show the 1σ error bars for each sample indicating the error of prediction. Note that the sample-specific error is high and generally higher than the overall temperature changes estimated for the individual core (Fig. 5). However, the regular trends shown by each core in combination with their overall similarity indicate that the calculations are reliable. We note, in particular, the similar pattern during the deglaciation with rapidly rising temperatures during Heinrich stadial HS1 and the Bølling and Allerød interstadials. The bottom water temperatures are generally slightly colder in the two cores from the southern part of through, where water depth was slightly shallower (Fig. 1; Table 1).

Table 2
AMS-^{14}C dates and calibrated dates for the investigated 12 from Storfjorden and Storfjorden Trough.

Core	Depth cm	14C -age	Calender age	Lab. Code	Species	References
STEP16-K01	110.5	1920 ± 22	1470 ± 42	UB41070	*Nucula* sp.	This study
	204	2603 ± 22	2300 ± 32	UB41071	*Portlandia* fragments	This study
	410.5	4894 ± 24	5243 ± 47	UB41072	*Nucula* sp.	This study
	498.5	5919 ± 27	6328 ± 37	UB41073	*Corbula gibba*	This study
	564.5	6755 ± 29	7281 ± 36	UB41074	*Bulla* sp.	This study
	705.5	8230 ± 31	8726 ± 77	UB41075	*Yoldiella* sp.	This study
	805.5	9158 ± 38	9955 ± 88	UB39427	Nucula sp.	This study
	880.5	9574 ± 35	10,453 ± 60	UB39426	Yoldiella sp.	This study
	937.5	10,358 ± 34	11,353 ± 105	UB39425	Nucula sp.	This study
JM10-10 GC	44.5	832 ± 21	473 ± 20	UB-17204	*Nucula* sp.	Rasmussen and Thomsen (2014)
	102.5	1491 ± 22	1029 ± 43	UB-17205	*Nuculana* sp.	Rasmussen and Thomsen (2014)
	136.5	3008 ± 27	2770 ± 32	UB-17206	*Astarte* sp.	Rasmussen and Thomsen (2014)
	210.5	4182 ± 41	4278 ± 73	UB-18845	*N. labradorica*	Rasmussen and Thomsen (2014)
	250.5	4573 ± 28	4805 ± 34	UB-18946	*N. labradorica*	Rasmussen and Thomsen (2014)
	324–326	6065 ± 31	6482 ± 49	UB-17207	Bivalve	Rasmussen and Thomsen (2014)
	325	5990 ± 43	6398 ± 57	UB-21198	*N. labradorica*	Rasmussen and Thomsen (2014)
	345–346	9778 ± 40	10,678 ± 64	UB-18947	Bivalve	Rasmussen and Thomsen (2014)
	385–386	10,960 ± 44	12,532 ± 55	UB-18948	Bivalve	Rasmussen and Thomsen (2014)
NP05-86 GC	28.5	1212 ± 32	744 ± 42	AAR-10854	*Cylichna* sp.	Rasmussen and Thomsen (2014)
	110.5	3371 ± 39	3242 ± 61	AAR-10918	Gastropod	Rasmussen and Thomsen (2014)
	140.5	4593 ± 46	4818 ± 48	AAR-10739	Ophiurian ossicles	Rasmussen and Thomsen (2014)
	224.5	8305 ± 50	8875 ± 88	AAR-10919	*Nucula* sp.	Rasmussen and Thomsen (2014)
	257.5	9685 ± 55	10,582 ± 69	AAR-10740	*N. labradorica*	Rasmussen and Thomsen (2014)
	269.5	10,395 ± 60	11,459 ± 156	AAR-10920	*Nuculana* sp.	Rasmussen and Thomsen (2014)
JM10-12 GC	31.5	1275 ± 23	825 ± 43	UB-17208	*Portlandia arctica*	Rasmussen and Thomsen (2014)
	75.5	3513 ± 27	3398 ± 36	UB-21669	Molluscs	Rasmussen and Thomsen (2014)
	212–214	9970 ± 45	10,802 ± 90	UB-17209	*Nuculana*	Rasmussen and Thomsen (2014)
	305–306	11,160 ± 81	12,660 ± 65	UB-21671	Foraminifera, molluscs	Rasmussen and Thomsen (2014)
HH12-1209 GC	15.5	modern'	<1950 A.D.	UB-24643	*Thyasira* sp.	Rasmussen and Thomsen (2014)
	75.5	2034 ± 25	1592 ± 45	UB-24644	*Portlandia arctica*	Rasmussen and Thomsen (2014)
	99.5	6894 ± 37	7750 ± 50	UB-25883	*Nucula* sp.	Rasmussen and Thomsen (2014)
	127.5	9750 ± 48	10,644 ± 65	UB-24645	*Nucula* sp.	Rasmussen and Thomsen (2014)
	171.5	10,568 ± 43	11,866 ± 106	UB-24646	*Nuculana* sp.	Rasmussen and Thomsen (2014)
	219.5	12,953 ± 53	14,038 ± 76	UB-24647	*Thyasira* sp.	Rasmussen and Thomsen (2014)
	243.5	13,105 ± 66	14,248 ± 157	UB-25612	Foraminifera, molluscs	Rasmussen and Thomsen (2014)
HH12-1212 GC	41.5	1352 ± 25	904 ± 33	UB24648	*Portlandia arctica*	Nielsen and Rasmussen (2018)
	132.5	3944 ± 28	3925 ± 49	UB24649	*Nucula* sp.	Nielsen and Rasmussen (2018)
	196.5	7899 ± 38	8362 ± 35	UB24651	*Portlandia* fragment	Nielsen and Rasmussen (2018)
	241.5	Failed		UB-24652	*N. labradorica*	Nielsen and Rasmussen (2018)
	245.0	12,340 ± 57	13,814 ± 82	UB-25132	Bryozoan	Nielsen and Rasmussen (2018)
	300.5	Failed		UB-25611	*Elphidium excavatum*	Nielsen and Rasmussen (2018)
	299–303	13,171 ± 49	15,207 ± 74	UB-28381	*E. excavatum, macrofossils*	Nielsen and Rasmussen (2018)
HH14-004 GC	114–117	8136 ± 41	8600 ± 63	UB28245	*Bathyarca glacialis*	This study
	230–232	12,463 ± 59	13,944 ± 84	UB28246	*Astarte* sp., *Nucula*	This study
	342–343	13,277 ± 54	15,350 ± 116	UB28247	*Nuculana pernula*	This study
HH16-564 GC	104.5	13,075 ± 50	15,097 ± 102	AAR28068	*Nucula, Portlandia*	This study
	228.5	13,331 ± 48	15,434 ± 116	AAR28069	*Portlandia arctica*	This study
HH15-1282 GC	20	7730 ± 39	8209 ± 54	UB31783	*Thyasira* sp.	This study
	150	13,042 ± 47	15,040 ± 111	UB31784	*Nucula*, *Nuculana*	This study
	180	13,205 ± 56	15,239 ± 89	UB34650	*Yoldiella*	This study
	242–244	13,434 ± 80	15,591 ± 157	UB35152	Bivalves, Scaphopod	This study
	274	13,354 ± 58	15,466 ± 128	UB34651	*Nucula* spp	This study
HH16-567 GC	16.5	modern'	<1950 A.D.	AAR28065	*Nucula* sp.	This study
	70.5	8014 ± 60	8465 ± 65	UB35154	*Nucula*, foraminifera	This study
	88.5	8654 ± 32	9336 ± 50	AAR28066	*Nucula, Nuculana, Thyasira*	This study
	228.5	14,139 ± 51	16,578 ± 133	AAR28067	Vesicomyid bivalve	This study
HH15-1288 GC	63	6244 ± 34	6690 ± 44	UB31784	*Nuculana* sp.	This study
	129.5	12,748 ± 55	14,318 ± 166	UB34707	*Nucula* sp.	This study
	239.5	13,090 ± 56	15,118 ± 103	UB34708	*Thyasira*, bryozoans, ostracods	This study
	259.5	13,102 ± 59	15,135 ± 59	UB34709	*Thyasira*, *Nucula* sp.	This study
	271.5	14,456 ± 58	17,079 ± 114	UB36056	*N. pachyderma* s	This study
JM02-460 GC	20	880 ± 55	497 ± 41	AAR-8915	Bivalve	Rasmussen et al. (2007)
	90	2570 ± 60	2239 ± 74	AAR-8916	Foraminifera	Rasmussen et al. (2007)
	160	4645 ± 50	4871 ± 57	Tua-3975	Bivalves	Rasmussen et al. (2007)
	210	7780 ± 65	8248 ± 69	AAR-8917	Benthic foraminifera	Rasmussen et al. (2007)
	280	10,655 ± 140	12,035 ± 299	Tua-3976	Foraminifera, molluscs	Rasmussen et al. (2007)
	340–345	12,890 ± 110	14,677 ± 287	AAR-8918	Bivalve, gastropod	Rasmussen et al. (2007)
	375	13,180 ± 140	15,254 ± 254	Tua-3977	Bivalve	Rasmussen et al. (2007)
JM02-460 PC	406	13,450 ± 90	15,612 ± 170	AAR-8762	*Nuculana* sp.	Rasmussen et al. (2007)
	413	15,250 ± 130	18,070 ± 116	AAR-9448	*N. pachyderma s*	Rasmussen et al. (2007)
	451.5	15,950 ± 110	18,793 ± 106	AAR-8763	*N. pachyderma s*	Rasmussen et al. (2007)
	463	16,750 ± 110	19,730 ± 149	AAR-8764	*N. pachyderma* s	Rasmussen et al. (2007)

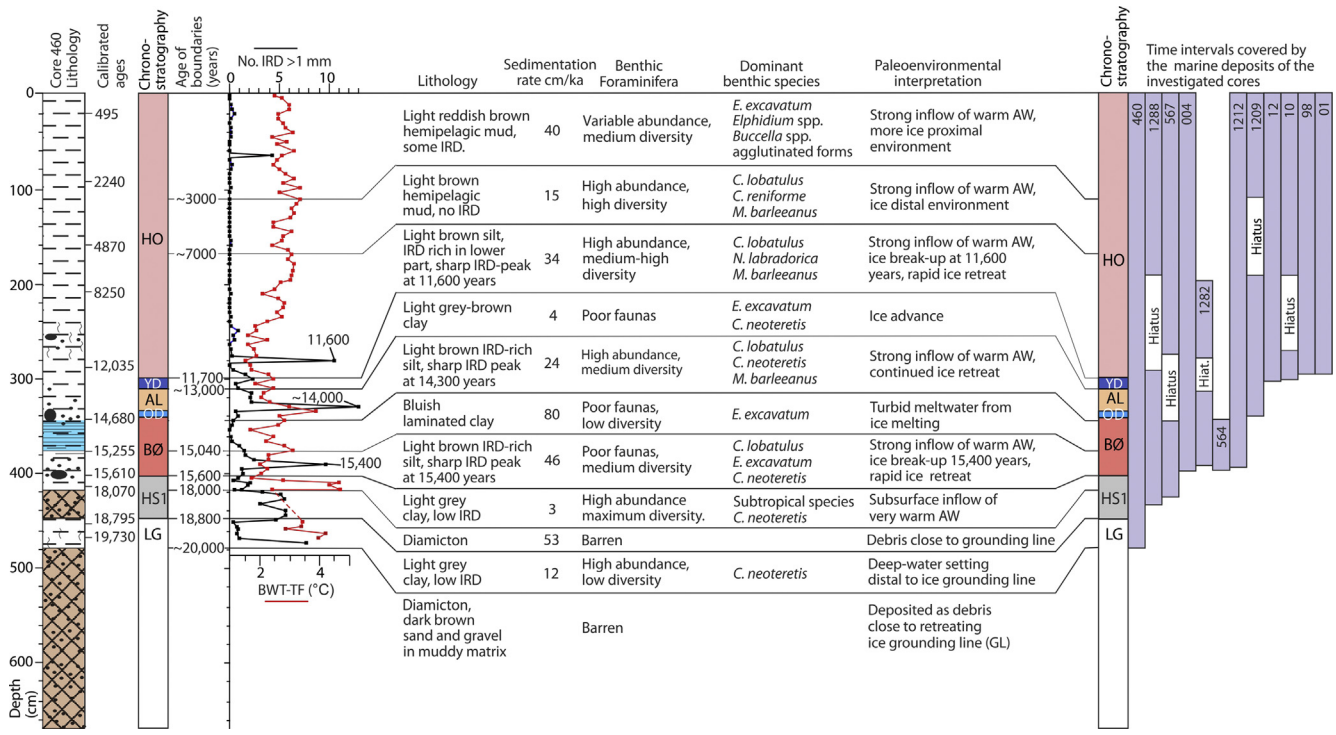

Fig. 4. Summary of lithology, distribution of benthic and planktic foraminifera and paleoenvironment from late glacial to early Holocene in Storfjorden Trough/Storfjorden. Lithology and stratigraphy from reference core 460 are indicated in columns to the right. Chronostratigraphic distribution of the marine sediments of the 12 investigated cores are shown to the right. Abbreviations and legend as in Fig. 2.

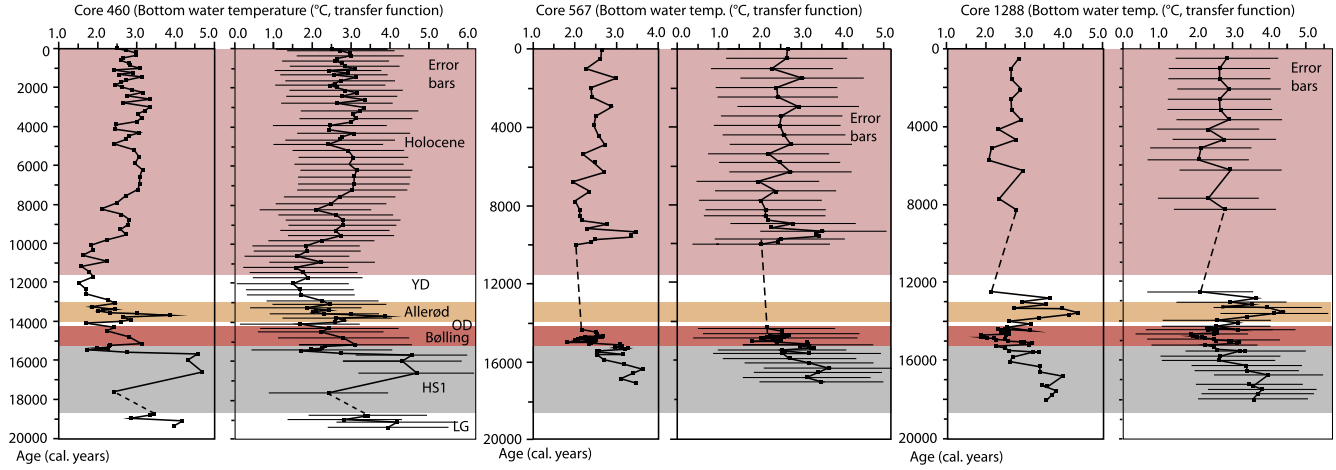

Fig. 5. Bottom water temperatures estimated by transfer functions for cores 460, 567 and 1288 plotted versus time in calendar years BP. For each core we show the temperatures with (right) and without error bars (left).

4. Discussion

4.1. Ice movements in Storfjorden Trough/Storfjorden from late LGM to early Holocene

4.1.1. Late glacial Maximum and Heinrich stadial HS1 (~20,000–15,600 years)

From 27,000 to 21,000 years, the ice margin of the western Svalbard-Barents Sea Ice Sheet was at the shelf edge (Elverhøi et al., 1995; Landvik et al., 1998; Ingólfsson and, Landvik, 2013; Hughes et al., 2016). This conclusion is supported by the total absence of marine sediments from this period in any of the investigated cores (Fig. 2). Ice-retreat in the Storfjorden Trough area must have begun shortly after 21,000 years as indicated by a dating of ~20,000 years for the appearance of foraminifera-rich sediments in the westernmost core 460 (Figs. 1 and 2). During the following period from ~20,000 to 15,600 years, the ice front moved back and forth close to grounding zone G4 as revealed in core 460, where the foraminifera-rich deposits from 18,800 to 18,100 years are replaced by a diamicton almost devoid of foraminifera (Rasmussen et al., 2007) (Figs. 2, 3 and 6). The re-establishment of rich foraminiferal faunas in core 460 at 18,100 years compares well with datings of 18,200 and 17,100 years of a similar foraminifera-rich environment in cores 1288 and 567 from the southern part of the trough in front of G4 (Figs. 1 and 2). We therefore conclude that at ~18,000 years in the beginning of Heinrich stadial HS1, the ice front had retracted to G4 (Figs. 1 and 6).

Paleoenvironmentally, Heinrich stadial HS1 is characterized by a strong contrast between warm bottom water conditions and cold surface water (Fig. 3). The relatively warm bottom water is indicated by a

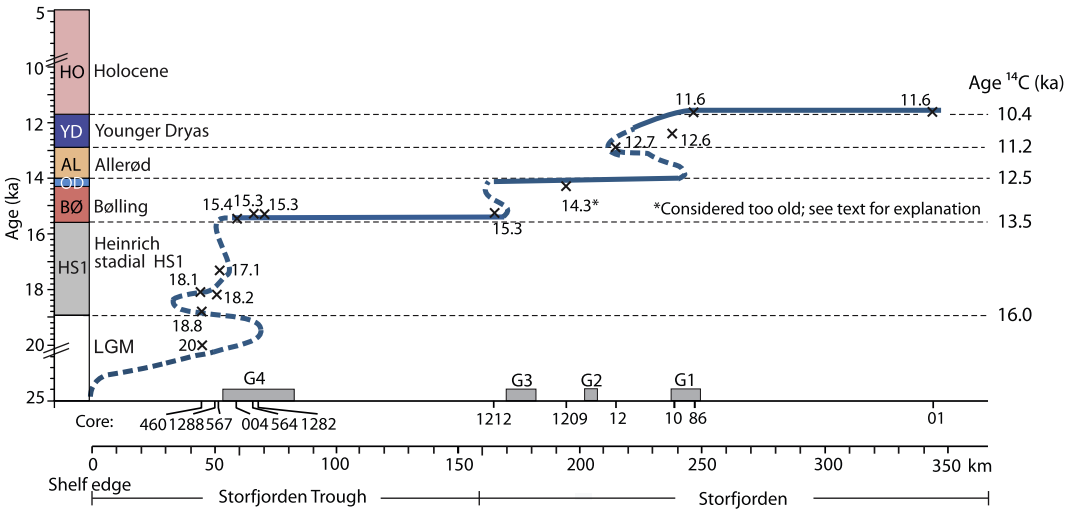

Fig. 6. Reconstruction of ice retreat in Storfjorden Trough/Storfjorden. Time-distance diagram indicating ice movements in Storfjorden Trough/Storfjorden comprising the period from the late LGM to early Holocene (~20,000–11,600 years). Bars labelled G1–G4 mark position of grounding zones. Core locations and dates of oldest hemipelagic sediments in each core (in calendar and ^{14}C ka) are indicated.

substantial proportion of the warm "Atlantic species group" (Rasmussen et al., 2007) and by temperatures of up to 4.5 °C estimated by transfer functions on the basis of the benthic foraminiferal faunas (Figs. 2–5). Heinrich stadial HS1 bottom water temperatures and salinities are the highest for the entire 460 record (Figs. 3 and 5). Bottom water temperatures in cores 567 and 1288 also show high values during HS1 (Fig. 5).

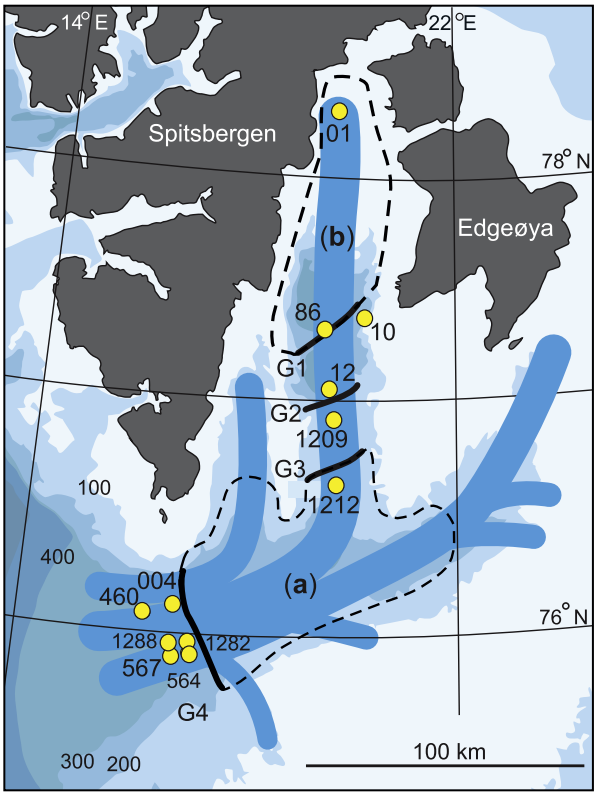

Fig. 7. Map of Storfjorden Trough and Storfjorden with core locations, grounding lines, and the three main ice-streams indicated (in this study collectively termed the 'Storfjorden Ice Stream'. Base map is modified from Rasmussen and Thomsen (2014) and Fig. 1, this study). Stippled lines mark parts of ice sheets estimated to have broken off during (a) early Bølling interstadial and (b) early Holocene interglacial. The early Bølling disintegration (~11,000 km^2) follows roughly the 150–200 m contour line. The early Holocene disintegration (4500 km^2) follows roughly the 80 m contour line. The Storfjorden Ice Stream during Heinrich stadial HS1 is estimated to have occupied and area of about 35,000 km^2. Size of areas are estimated applying the Google Earth area calculator tool.

The total dominance of the polar foraminiferal species *Neogloboquadrina pachyderma* s together with low planktic $\delta^{18}O$ values indicate that surface waters were cold and covered by a layer of meltwater (Fig. 3). Altogether, we conceive a water column during Heinrich stadial HS1 with warm Atlantic water flowing north along the bottom of the trough below a layer of cold, icy surface water (see also Rasmussen et al., 2007) (Figs. 3 and 5).

4.1.2. The deglaciation period from Bølling to early Holocene (15,600–11,600 years)

The next major event in the trough area is the retreat of ice from grounding zone G4 (Fig. 6). Datings of 15,400, 15,300 and 15,300 years of the oldest marine sediments in cores 004, 564 and 1282 taken within the grounding zone indicate that the retreat occurred close to the base of the Bølling interstadial. The retreat coincides in time with a warming of the bottom water, a substantial increase in ice rafting and an abrupt warming of the atmosphere over Greenland (Figs. 3, 5 and 6). The average age, 15,335 years, of the retreat from the three cores from grounding zone G4 is practically inseparable from the age of the oldest marine deposits in core 1212 (15,300 years) taken in front of grounding zone G3 at the mouth of Storfjorden >125 km away (Figs. 1 and 6). This suggests that the outer >125 km of the ice-stream comprising an area of ~11,000 km^2 broke away and disintegrated nearly instantaneously (Fig. 7). The presence of a macro- and microfauna in the diamictic/glacimarine sediments of cores 1212, 1282 and 564 indicate that most of the ice sheet had lifted off before the final collapse (see also Nielsen and Rasmussen, 2018). The faunas are fairly species rich although of low abundance (see Nielsen and Rasmussen, 2018) (Figs. 1 and 2).

However, considering the dating errors (Table 2), we cannot exclude the possibility of a modest time delay between the break-up at grounding zones G4 and G3. In order to examine this possibility, we have analyzed the distribution of IRD (ice rafted debris) in the three cores (460, 567 and 1288) taken in front of grounding zone G4 (Figs. 1 and 2). High concentrations of IRD in marine sediments reflect presence of numerous melting icebergs at the sea surface (Ruddiman, 1997). In all three cores, we notice a distinct maximum of IRD in the early part of the Bølling interstadial (Figs. 2 and 3). Peak deposition seems to have occurred over a period of less than 50 years. In cores 460 and 567, the peak is dated to 15,300 years. In 1288, it is somewhat younger dated to around 15,130 years. It is equally important for our understanding of the early Bølling events that IRD is virtually absent in the strongly laminated bluish clay that from ~15,255/15,040–14,600 years was deposited on the shelf and slope throughout western Svalbard (Elverhøi et al., 1995; Birgel and Hass, 2004; Jessen et al., 2010) (Figs. 2–4). The IRD-free, laminated clay is a hemipelagic meltwater deposit and its appearance in grounding zone G4 indicate that the outer part of the Storfjorden Ice Stream had now completely disappeared (Figs. 1 and 2). The development in the Storfjorden Trough thus supports our previous conclusion that the break-up of the Storfjorden Ice Stream was extremely fast.

The disappearance of the outer part of Storfjorden Ice Stream coincides with the abrupt atmospheric warming seen in Greenland ice cores at the beginning of the Bølling interstadial (Fig. 3). Along the coast of Svalbard, the warming is connected to a strong subsurface intrusion of Atlantic water, and conditions similar to those in Storfjorden have been recorded in several well-dated cores from the western and northern Svalbard shelf and slope and with similar timing (e.g., Svendsen et al., 1996; Landvik et al., 2005; Ślubowska-Woldengen et al., 2007; Rasmussen et al., 2007; Jessen et al., 2010; Falardeau et al., 2018; Ivanova et al., 2019). At the surface, planktic foraminifera are nearly absent probably due to the presence of turbid meltwater run-off from the Svalbard-Barents Sea Ice Sheet (Rasmussen et al., 2007) and it has not been possible to calculate sea surface temperatures (Fig. 3).

In core 460, we find two further incidences of abrupt increase in the concentration of IRD during the deglaciation. The first occurs shortly after the beginning of the Allerød interstadial and is dated to ~14,000 years; the second occurs at the beginning of the Holocene and dated to 11,600 years (Figs. 2–4). Both peaks are associated with increased inflow of Atlantic water to the Nordic Seas and Svalbard margin (Elverhøi et al., 1995; Birgel and Hass, 2004; Aagaard-Sørensen et al., 2010; Falardeau et al., 2018 and references therein) and rapid atmospheric warming (Johnsen et al., 1992; Rasmussen et al., 2014). They are also linked to higher ice retreat rates in the Storfjorden Ice Stream (Fig. 6). However, the ice movements during the Allerød and Younger Dryas are relatively poorly documented because of few dates. From cores 1288, 004, and 1212 we obtain ages for the Older Dryas-Allerød transition of c. 14,320, 13,945 and c. 13.815 years, respectively. The average of these ages is 14, 026 years, which is close to the age of the basal Allerød event in the Nordic and Barents seas dated to 14,000 years (see above). Nielsen and Rasmussen (2018) dated the diamicton-marine transition in core 1209 to 14,300 years based on microfossils interpreted as belonging to the early Allerød interstadial (Fig. 2, Table 2). The tentative reconstruction presented in Fig. 6 for Allerød interstadial and Younger Dryas stadial is based on the average date presented above, and dates in core 12 of 12,700 years and core 10 of 12,600 years (Fig. 2). It should be noted that Nielsen and Rasmussen (2018) suggested that the ice-stream retreated about 60 km at the start of the Allerød interstadial concomitant with the Allerød warming (Figs. 3 and 5) and advanced at least 20 km during the Younger Dryas cooling between ~13,000 and 11,700 years (Fig. 6).

The early Holocene collapse of the ice-stream occupying the inner part of Storfjorden between cores 86 and 01 was probably also instantaneous, as the oldest glacimarine sediments in both cores date 11,600 years (Figs. 1–4, 6). The ice-stream retreated at least 100 km and lost an area of ~4500 km^2 (Fig. 7). Similar to the start of the Bølling Interstadial, the ice had probably lifted-off its base before the rapid disintegrations. This is indicated by the appearance of a species-rich benthic foraminiferal fauna immediately above the diamictons (Rasmussen and Thomsen, 2014, 2015) (Fig. 2).

The early Holocene datings carries the same uncertainties as the Bølling dates, but the very uniform sedimentation rates in the two records lends strong credence to the age models of the two cores (Fig. 2, Table 2) (see also discussion below). It is also necessary to comment on the reservoir age in Storfjorden during the early Holocene. Cores 86 and 01 are today situated in relatively shallow water (Table 1) and it could be argued that the reservoir age here differed from the reservoir age in the outer and deeper parts of the fjord. However, the present water depth at the two core sites is the result of an isostatic uplift of more than 80 m since the early Holocene (Bondevik et al., 1995; Forman et al., 2004; Tian et al., 2020). Water depth during the early Holocene was therefore much deeper than it is today. This suggests that the reservoir age at the time of the ice collapse were the same throughout Storfjorden and probably close to the present global standard as recorded in coastal southwestern Norway (Bondevik et al., 2006).

In Storfjorden Trough and Storfjorden, both disintegration events correlate with extraordinary rapid climatically driven sea-level rises; meltwater peak Mwp1A shortly after the start of Bølling and Mwp1B at the start of Holocene (Fairbanks, 1989). During early Bølling, the sea level rose 14–18 m in ~350 years with peak rises of more than 4.3 cm/year (Deschamps et al., 2012). The early Holocene sea-level rise was of a similar magnitude as the Bølling rise (Abdul et al., 2016; Tian et al., 2020). By lifting the ice on the continental margin, the sea level rises may have played a decisive role for the rapid collapses of the Storfjorden Ice Stream during the early Bølling and early Holocene, similar to the role it apparently played for the rapid break-down of the Irish Sea ice sheet during the same period (Ó Cofaigh et al., 2019).

It is evident from this result and from several earlier studies that the collapses of Storfjorden Ice Stream coincide with a strong warming of the Norwegian and Svalbard margins caused by increased inflow of warm Atlantic surface water to the Nordic seas and Svalbard margin (e.g., Lehman et al., 1992; Koc and Jansen, 1992; Vorren and Plassen, 2002; Ślubowska-Woldengen et al., 2007; Aagaard-Sørensen et al., 2010; Falardeau et al., 2018 and references therein) (Figs. 3 and 5). It is also evident that the collapses follow shortly after major atmospheric

warmings as indicated by the correlation to the Greenland ice cores (see above) (Fig. 3).

4.2. Synchronous ice movements of the western Barents Sea ice sheet from Svalbard in the north to northern Norway in the south

In order to obtain a more regional perspective we correlate our results from Storfjorden and Storfjorden Trough with data from the north Norwegian margin (Junttila et al., 2010; Aagaard-Sørensen et al., 2010) and four Norwegian fjords (Vorren and Plassen, 2002) all located 700–800 km south of Storfjorden. The retreats and advances in Storfjorden Trough during late LGM and Heinrich stadial HS1 are overall synchronous with the retreats and advances described from Andfjorden, northern Norway (Vorren and Plassen, 2002) (Figs. 6 and 8). In both Storfjorden Trough and Andfjorden, the ice had withdrawn from the shelf margin at ~20,000 years. On both margins, we notice an advance between 19,000 and 18,000 years followed by a retreat from ~18,000 years and a smaller re-advance before the beginning of the Bølling Interstadial at 15,600 years (Figs. 6 and 8). Vorren and Plassen's (2002) dating of the beginning of HS1 to 19,000 years is also similar to our dating in core 460 (Figs. 2 and 3). A notable difference is that the ice retreat after 18,000 years was much wider and faster on the north Norwegian margin (Vorren and Plassen, 2002; Junttila et al., 2010), than on the Storfjorden margin, where it was small and slow (Figs. 6 and 8).

Focusing on ice movements during the Bølling and Allerød Interstadials, we observe the same sequence of depositional environments in northern Norway as on the western slope of Svalbard and, furthermore, with similar chronology. The sequence comprises an early Bølling IRD peak followed by a laminated unit and a second peak of IRD; the latter is referred to the Allerød Interstadial (Aagard-Sørensen et al., 2010; Junttila et al., 2010) (Figs. 2 and 3). The early Bølling IRD peak in the southern Barents Sea is dated to 15,300, which is exactly the same date as in core 460 from the Storfjorden Trough. The IRD peaks signify the early disintegration of ice streams of the Svalbard-Barents Sea Ice Sheet and is a response to the early Bølling warming (Figs. 2, 3 and 6). The laminated layer dates to 15,040–14,600 years on the Svalbard margin (Birgel and Hass, 2004; Jessen et al., 2010; this study). It was probably deposited from turbid meltwater run-off produced by the now rapidly melting and thinning Svalbard-Barents Sea Ice Sheet (Figs. 2 and 6). The presence of laminated beds of the same age on the Bjørnøya Fan (Danielsen, 2017) between Norway and Svalbard suggests that the formation of sediment-loaded meltwater was not a local phenomenon limited to the land-near localities (Fig. 1). The increased ice rafting from the beginning of the Allerød interstadial at 14,000 years on both the Svalbard and north Norwegian margin (e.g., Junttila et al., 2010; Aagaard-Sørensen et al., 2010; Jessen et al., 2010) may have been enhanced by an advance of the ice sheet during the preceding cold Older Dryas stadial (Fig. 2). We note that IRD disappeared in the records from the shelf of northern Norway from the end of the Younger Dryas ~11,700 years, while it continued or increased in the records from Storfjorden Trough and the Svalbard margin into the early Holocene until ~10,500 years (Ślubowska et al., 2005; Ślubowska-Woldengen et al., 2007; Jessen et al., 2010) (Figs. 2 and 3).

Analyzing retreat and advances, we compare our results with time-distance data from four north Norwegian fjords (Andfjorden, Malangen, Lyngen and Altafjorden) published by Stokes et al. (2014). They apply the stratigraphy and age model of Vorren and Plassen (2002), just as they use their data from Andfjorden. Stokes et al. (2014) investigated four additional fjords from northern Norway, but as they behave very similarly to the ice stream in Altafjorden they are not discussed here.

The correlation reveal a remarkable similarity between the Storfjorden Ice Stream and the four Norwegian ice streams (Fig. 8). In both areas, the major retreats and the highest retreat rates occur at the start of the Bølling and Allerød Interstadials and Holocene Interglacial. But there are also some differences. Thus, the retreat pattern during the early Holocene is stepwise in the Norwegian fjords probably reflecting that the ice streams are now far inland and confined to the inner, narrower parts of the fjords (Åkesson et al., 2018) (Fig. 8). However, the similar timing of the largest and fastest retreat on the two margins clearly indicate that the main controlling forces were the same. As the major retreats coincides with the warming events at the start of the Bølling and Allerød interstadials and early Holocene interglacial, we conclude that these forces were the global atmospheric and oceanic warming. Our interpretation of the development in the Norwegian fjords is in stark contrast to Stokes et al.'s (2014) own interpretation. The found that retreats and advances in the Norwegian streams were primarily controlled by ground topography and water depth and not directly linked to climate (see Fig. 8 for explanation).

4.3. The dynamics of the Storfjorden Ice Stream compared to modern ice retreats

The disintegration of the Storfjorden Ice Stream shows many similarities to the recent disintegration of most of the Larsen Ice Shelf, Antarctica (Fig. 7). The Larsen Ice Shelf broke up between 1995 and 2017 and a total 10,600 km^2 of shelf ice disappeared (Scambos et al., 2004; Cook and Vaughan, 2010; Hogg and Gudmundsson, 2017). Like the Storfjorden Ice Stream, the Larsen Ice Sheet is floating allowing for the intrusion of warm water below the ice. Accepting the dating uncertainties for the oldest marine sediment in each core, and given the overall temporal resolution of the study, we suggest a time-frame for the break-up ranging from nearly instantaneous to about 50–100 years. This corresponds to a retreat rate of 2.5 km/year for the Bølling transition and 2 km/year for the Holocene transition. These values are also comparable with a number of recent rates measured in Antarctica of 0.6–>2 km/year (e.g., Scheugl et al., 2016; Konrad et al., 2018 and references therein) and in Greenland (e.g., Howat et al., 2007; Holland et al., 2008; Luckman et al., 2006), and also with deglacial retreat rates calculated for the ice sheet of the northern North Sea (Bradwell et al., 2020) and the Irish Ice Sheet (Small et al., 2018).

It has previously been suggested that subsurface warming was the main cause for the rapid retreat and break-up of the ice streams during the last glacial and deglaciation periods (Rasmussen and Thomsen 2004; Marcott et al., 2011; Ezat et al., 2014). A recent model study of the deglaciation of the Svalbard-Barents Sea Ice Sheet reaches similar conclusions (Petrini et al., 2020). Numerous modern studies indicate that incursion of subsurface warm water underneath ice shelves and outlet glaciers have accelerated the disintegration of marine-based ice in both Greenland (e.g., Luckman et al., 2006; Holland et al., 2008; Howat et al., 2010; Bjørk et al., 2012) and Antarctica (e.g., Jacobs et al., 2011; Rintoul et al., 2016; Jeong et al., 2016; Hogg et al., 2017; Konrad et al., 2018). Together with atmospheric warming, this incursion constitute the major forcings for the recent increase in ice calving and melting.

5. Conclusions

The Storfjorden Ice Stream was a 350 km long composite ice stream that during the coldest parts of the last glaciation occupied the present Storfjorden and Storfjorden Trough, southwestern Svalbard. The ice stream covered an area of more than 35,000 km^2. During the late LGM and Heinrich stadial HS1, the front of the stream was relatively stable moving back and forth on the outer shelf over a distance of less than 50 km. From the beginning of the Bølling interstadial, this situation was replaced by a pattern dominated by rapid retreats and at the beginning of the Holocene, the ice stream had completely vanished.

The retreat was not uniform over time. About haft of the ice disappeared in two almost instantaneous collapses. The first occurred at the beginning of the Bølling interstadial, when more than 11,000 km^2 of ice sheet from Storfjorden Trough and the outer fjord disintegrated. The second collapse took place at the beginning of the early Holocene and comprised about 4500 km^2 of ice from the inner fjord system. During both break-ups, the ice front retreated about 100 km. Instant

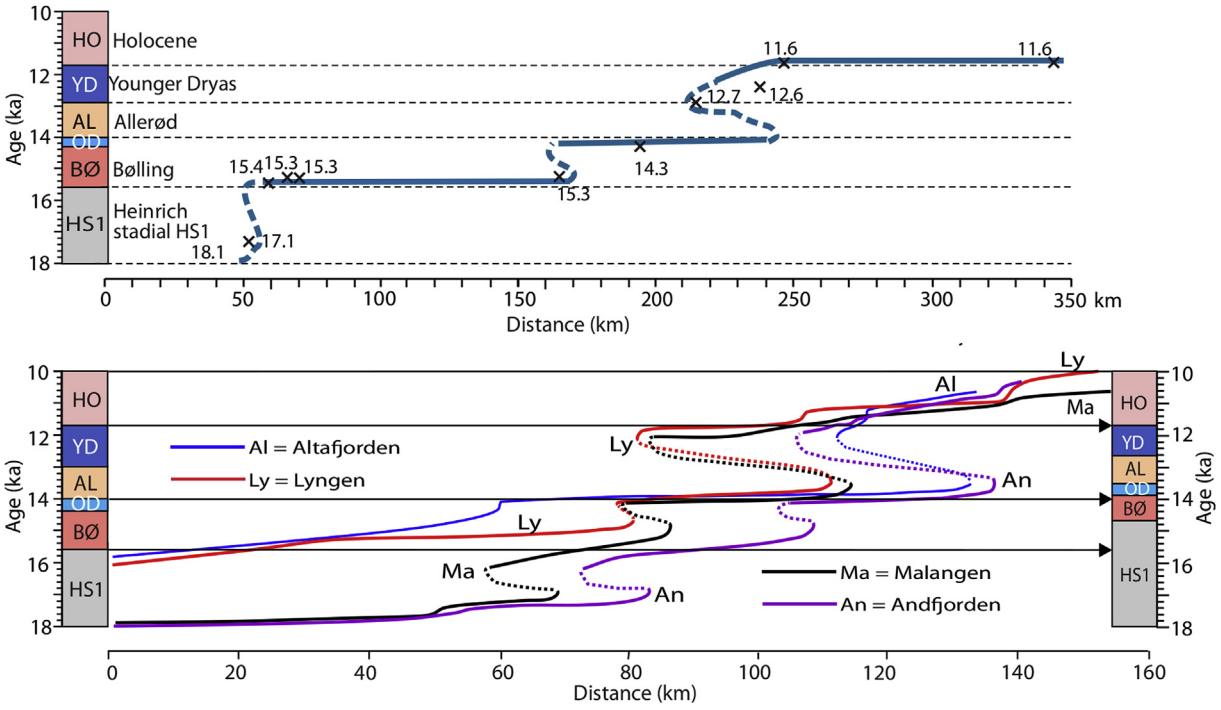

Fig. 8. Time-distance diagrams comparing ice movements in (a) Storfjorden Ice Stream with movements in (b) four north Norwegian ice streams (from Stokes et al., 2014). Column to the right shows the marine chronostratigraphy of Vorren and Plassen (2002) and this study, column to the left show the chronostratigraphy of Stokes et al. (2014). The major retreats and highest retreat rates in all ice streams occur during the main warming phases of Bølling and Allerød Interstadials and early Holocene Interglacial. After using the marine stratigraphy and marine ages for the reconstruction of ice movements, Stokes et al. (2014) chose to use ice core ages for the climate signal; that is 14,700 years for the start of the Bølling warming instead of 15,600 years, and 13,500 years for the start of the Allerød warming instead of 14, 000 years (marked by arrows), thus creating a mismatch between the timing of the ice movements and the timing of the temperature curve. We believe that the mixing of marine and ice core chronostratigraphy is the main reason for why Stokes et al. (2014) finds that non-climatic factors like topography and water depth are more important than climatic in controlling retreats and advances of marine terminating glaciers.

disintegration is the most likely scenario for the early Bølling and early Holocene collapses. However, taking account for the dating uncertainties the collapse may have taken longer time possibly up to 50 years corresponding to retreat rates of ~2 km per year. During the Allerød Interstadial and Younger Dryas periods, the Storfjorden Ice Stream experienced both retreat and re-advance creating hiati in the sedimentary records. Exact calculations of retreat rates for these periods have therefore not been possible.

The early Bølling and early Holocene collapses of the Storfjorden Ice Stream coincide with the most important global temperature increases during the deglaciation and we are confident that the collapses were forced by climatic and oceanographic warmings. These warming events are accompanied by rapid global sea level rises. Micropaleontological evidence indicate that the Storfjorden Ice Stream was lifted-off its base and became floating, which undoubtedly, contributed to the rapid disintegration.

Our data indicate that the retreat pattern of the Storfjorden Ice Stream correlate in time with the retreats patterns previously described from several north Norwegian fjords. This implies that the ice movements in these fjords also were chiefly controlled by climate, and not as previously suggested by local factors such as water depth and bottom topography. Altogether, we conclude that ice retreat in the Atlantic region at high northern latitudes was controlled by climate and ocean warmings.

Author contribution

TLR performed the new analyses and wrote the first draft together with ET. TLR and ET rewrote and edited together and discussed data and results.

Declaration of competing interest

The authors declare that they have no known competing financial interests or personal relationships that could have appeared to influence the work reported in this paper.

Acknowledgement

We thank the captains and crews, shipboard scientific parties, students, and engineer Steinar Iversen for help with core retrievals during cruises with RV *Jan Mayen/Helmer Hanssen* (UiT the Arctic University of Norway) in 2002–2016 and RV *l'Atalante* (IFREMER) in 2016. Anders Solheim, Norwegian Geotechnical Institute, NGI, Oslo, Norway is warmly thanked for the figure (Fig. 1B and C) showing the seismic and acoustic data from UNIS AG202/AG216 cruise with RV *Jan Mayen* in 2002, when core 460 was taken. Jesper Olsen, Aarhus University supervised the datings of cores 564 and 567. This research was funded by UNIS 2002–2004 (University Centre in Svalbard), and TFS (Tromsø Forskningsstiftelse), UiT the Arctic University of Norway to the 'Paleo-CIRCUS' project 2010–2014. The project received further funding from 2013 from the Research Council of Norway through its Centres of Excellence funding scheme, project number 223259.

References

Aagaard-Sørensen, S., Husum, K., Hald, M., Knies, J., Paleoceanographic development in the SW Barents sea during the late Weichselian-early Holocene transition. Quat. Sci. Rev. 29, 3442–3456.

Abdul, N.A., Mortlock, R.A., Wright, J.D., Fairbanks, R.G., 2016. Younger Dryas sea level and meltwater pulse 1B recorded in Barbados reef crest coral *Acropora palmata*. Paleoceanography 31, 330–344.

Åkesson, H., Morlighem, M., Nisancioglu, K.H., Svendsen, J.I., Mangerud, J., 2018. Atmosphere-driven ice sheet mass loss paced by topography: insights from modelling the south-western Scandinavian Ice Sheet. Quat. Sci. Rev. 195, 32–47.

Birgel, D., Hass, H.C., 2004. Oceanic and atmospheric variations during the last deglaciation in the Fram Strait (Arctic Ocean): a coupled high-resolution organic-geochemical and sedimentological study. Quat. Sci. Rev. 23, 29–47.

Bjørk, A.A., Kjær, K.H., Korsgaard, N.J., Khan, S.A., Kjeldsen, K.K., Andresen, C.S., Box, J.E., Larsen, N.K., Funder, S., 2012. An aerial view of 80 years of climate-related glacier fluctuations in southeast Greenland. Nat. Geosci. 5, 427–432.

Björck, S., Kromer, B., Johnsen, S., Bennike, O., Hammarlund, D., Lemdahl, G., Possnert, G., Rasmussen, T.L., Wohlfarth, B., Hammer, C.U., Spurk, M., 1996. Synchronised terrestrial-atmospheric records around the North Atlantic. Science 274, 1155–1160.

Bond, G., Broecker, W.S., Johnsen, S.J., McManus, J., Labeyrie, L., Jouzel, J., Bonani, G., 1993. Correlations between climate records from North Atlantic sediments and Greenland ice. Nature 365, 143–147.

Bondevik, S., Mangerud, J., Birks, H.H., Gulliksen, S., Reimer, P., 2006. Changes in north Atlantic reservoir ages during the Allerød and younger Dryas. Science 312, 1514–1517.

Bondevik, S., Mangerud, J., Ronnert, L., Salvigsen, O., 1995. Postglacial sea-level history of Edgeøya and Barentsøya, eastern Svalbard. Pol. Res. 14, 153–180.

Bradwell, T., Small, D., Fabel, D., Clark, C.D., Chiverrell, R.C., Saher, M.H., Dove, D., Callard, S.L., Burke, M.J., Moreton, S.G., Medialdea, A., Bateman, M.D., Roberts, D.H., Colledge, N.R., Finlayson, A., Morgan, S., Ó Cofaigh, C., 2020. Pattern, style and timing of British-Irish ice sheet retreat: Shetland and northern North sea sector. J. Quat. Sci. https://doi.org/10.1002/jqs.3163.

Bradwell, T., Small, D., Fabel, D., Smedley, R.K., Clark, C.D., Saher, M.H., Callard, S.L., Chiverrell, R.C., Dove, D., Moreton, S.G., Roberts, D.H., Duller, G.A.T., Ó Cofaigh, C., 2019. Ice-stream demise dynamically conditioned by trough shape and bed strength. Sci. Adv. 5 https://doi.org/10.1126/sciadv.aau1380.

Brendryen, J., Haflidason, H., Yokoyama, Y., Haaga, K.A., Hannisdal, B., 2020. Eurasian ice sheet collapse was a major source of Meltwater Pulse 1A 14,600 years ago. Nat. GeoSci. https://doi.org/10.1038/s41561-020-0567-4.

Briner, J.P., Bini, A.C., Anderson, R.S., 2009. Rapid early Holocene retreat of a Laurentide outlet glacier through an Arctic fjord. Nat. Geosci. 2, 497–499.

Chistyakova, N.O., Ivanova, E.V., Risebrobakken, B., Ovsepyan, E.A., Ovsepyan, Y.S., 2010. Reconstruction of the postglacial environments in the southwestern Barents Sea based on foraminiferal assemblages. Oceanology 50, 573–581.

Cook, A.J., Vaughan, D.G., 2010. Overview of areal changes of the ice shelves on the Antarctic Peninsula over the past 50 years. Cryosphere 4, 77–98.

Danielsen, I.K., 2017. Paleoceanographic Development during the Last Deglaciation and Holocene, over the Bear Island Slide Scar, SW Barents Sea. Master Thesis. UiT, the Arctic University of Norway, Tromsø, Norway, p. 96. http://hdl.handle.net/10037/10615.

Davies, S.M., Wastegård, S., Rasmussen, T.L., Johnsen, S.J., Steffensen, J.P., Andersen, K.K., Svensson, A., 2008. Identification of the Fugloyarbanki Tephra in the NGRIP ice-core: a key tie-point for marine and ice-core sequences during the last glacial period. J. Quat. Sci. Rapid Commun. 23, 409–414.

Davies, S.M., Wastegård, S., Abbott, P.M., Barbante, C., Bigler, M., Johnsen, S.J., Rasmussen, T.L., Steffensen, J.P., Svensson, A., 2010. Tracing volcanic events in the NGRIP ice-core and synchronising North Atlantic marine records during the last glacial period. Earth Planet Sci. Lett. 294, 69–79.

Deschamps, P., Durand, N., Bard, E., Hamelin, B., Camoin, G., Thomas, A.L., Henderson, G.M., Okuno, J., Yokohama, Y., 2012. Ice-sheet collapse and sea-level rise at the Bølling warming 14,600 years ago. Nature 483, 559–564.

Duplessy, J.-C., Arnold, M., Maurice, P., Bard, E., Duprat, J., Moyes, J., 1986. Direct dating of the oxygen-isotope record of the last deglaciation by ^{14}C accelerator mass spectrometry. Nature 320, 350–352.

Elliot, M., Labeyrie, L., Bond, G., Cortijo, E., Turon, J.-L., Tisnerat, N., Duplessy, J.-C., 1998. Millennial-scale iceberg discharges in the Irminger Basin during the glacial period: relationship with the Heinrich events and environmental settings. Paleoceanography 13, 433–446.

Elverhøi, A., Andersen, E.S., Dokken, T., Hebbeln, D., Spielhagen, R., Svendsen, J.I., Sørflaten, M., Rørnes, A., Hald, M., Forsberg, C.F., 1995. Late quaternary sediment yield from the high Arctic Svalbard area. J. Geol. 103, 1–17.

Ezat, M., Rasmussen, T.L., Groeneveld, J., 2014. Persistent intermediate water warming during cold stadials in the southeastern Nordic seas during the past 65 k.y. Geology 42, 663–666.

Fairbanks, R.G., 1989. A 17,000-year glacio-eustatic sea level record:influence of glacial melting on the Younger Dryas event. Nature 342, 637–642.

Falardeau, J., de Vernal, A., Spielhagen, R.F., 2018. Paleoceanography of northeastern Fram Strait since the last glacial maximum: palynological evidence of large amplitude changes. Quat. Sci. Rev. 195, 133–152.

Forman, S.L., Lubinski, D.J., Ingólfsson, Ó., Zeeberg, J.J., Snyder, J.A., Siegert, M.J., Matishov, G.G., 2004. A review of postglacial emergence on Svalbard, Frnaz Josef land and Novaya Zemlya, northern Eurasia. Quat. Sci. Rev. 23, 1391–1434.

Hogan, K.A., Dowdeswell, J.A., Hillenbrand, C.-D., Ehrmann, W., Noormets, R., Wacker, L., 2017. Subglacial sediment pathways and deglacial chronology of the northern Barents Sea Ice Sheet. Boreas 46, 750–771.

Hogg, A.E., Gudmundsson, G.H., 2017. Impacts of the Larsen-C ice shelf calving event. Nat. Clim. Sci. 7, 541–542.

Hogg, A.E., Shepherd, A., Cornford, S.L., Briggs, K.H., Gourmelen, N., Graham, J.A., Joughin, I., Mouginot, J., Nagler, T., Payne, A.J., Rignot, E., Wuite, J., 2017. Increased ice flow in Western Palmer Land linked to ocean melting. Geophys. Res. Lett. 44, 4159–4167.

Holland, D.M., Thomas, R.H., de Young, B., Ribergaard, M.H., Lyberth, B., 2008. Acceleration of Jacobshavn Isbræ triggered by warm subsurface ocean waters. Nat. Geosci. 1, 659–664.

Howat, I.M., Box, J.E., Ahn, J., Herrington, A., McFadden, E.M., 2010. Seasonal variability in the dynamics of marine-terminating outlet glaciers in Greenland. J. Glaciol. 56, 601–613.

Howat, I.M., Joughin, I., Scambos, T.A., 2007. Rapid changes in ice discharge from Greenland outlet glaciers. Science 315, 1559–1561.

Hughes, A.L.C., Rainsley, E., Murray, T., Fogwill, C.J., Schnabel, C., Xu, S., 2012. Rapid response of Helheim Glacier, southeast Greenland, to early Holocene climate warming. Geology 40, 427–430.

Hughes, A.L.C., Gyllenkreutz, R., Lohne, Ø.S., Mangerud, J., Svendsen, J.I., 2016. The last Eurasian ice sheets – a chronological database and time-slice reconstruction, DATED-1. Boreas 45, 1–45.

Ingólfsson, Ó., Landvik, J.Y., 2013. The Svalbard-Barents Sea ice sheet - historical, current and future perspectives. Quat. Sci. Rev. 64, 33–60.

Ivanova, E., Murdmaa, I., de Vernal, A., Risebrobakken, B., Peyve, A., Brice, C., Seitkalieva, E., Pisarev, S., 2019. Postglacial paleoceanography and paleoenvironments in the northwestern Barents Sea. Quat. Res. 92, 430–449.

Jacobs, S.S., Jenkins, A., Giulivi, C.F., Dutrieux, P., 2011. Stronger ocean circulation and increased melting under Pine Island Glacier ice shelf. Nat. Geosci. 4, 519–523.

Jeong, S., Howat, I.M., Bassis, J., 2016. Accelerated ice shelf rifting and retreat at pine Island Glacier, west Antarctica. Geophys. Res. Lett. 43 (11), 720–11,725.

Jessen, S.P., Rasmussen, T.L., Nielsen, T., Solheim, A., 2010. A new Late Weichselian and Holocene marine chronology for the western Svalbard slope 30,000–0 cal years BP. Quat. Sci. Rev. 29, 1301–1312.

Johnsen, S.J., Clausen, H.B., Dansgaard, W., Fuhrer, K., Gundestrup, N., Hammer, C.U., Iversen, P., Jouzel, J., Stauffer, B., Steffensen, J.P., 1992. Irregular glacial interstadials in a new Greenland ice core. Nature 359, 311–313.

Johnsen, S.J., Dahl-Jensen, D., Gundestrup, N., Steffensen, J.P., Clausen, H.B., Miller, H., Masson-Delmotte, V., Sveinbjörnsdottir, A.E., White, J., 2001. Oxygen isotope and palaeotemperature records from six Greenland ice-core stations: camp Century, Dye-3, GRIP, GISP2, Renland and NorthGRIP. J. Quat. Sci. 16, 299–307.

Juggins, S., 2007. C2 Version 1.5 User Guide. Software for Ecological and Palaeoecological Data Analysis and Visualization. Newcastle University, Newcastle upon Tyne, UK.

Junttila, J., Aagaard-Sørensen, S., Husum, K., Hald, M., 2010. Late Glacial-Holocene clay minerals elucidating glacial history in the SW Barents Sea. Mar. Geol. 276, 71–85.

Koç, N., Jansen, E., 1992. A high-resolution diatom record of the last deglaciation from the SE Norwegian Sea: documentation of rapid climate changes. Paleoceanography 7, 499–520.

Konrad, H., Shepherd, A., Gilbert, L., Hogg, A.E., McMillan, M., Muir, A., Slater, T., 2018. Net retreat of Antarctic glacier grounding lines. Nat. Geosci. https://doi.org/10.1038/s41561-018-0082-z.

Kucera, M., Weinelt, M., Keifer, T., Pflaumann, U., Hayes, A., Weinelt, M., Chen, M.-T., Mix, A.C., Barrows, T.T., Cortijo, E., Duprat, J., Juggins, S., Waelbroeck, C., 2005. Reconstruction of sea-surface temperatures from assemblages of planktonic foraminifera: multi-technique approach based on geographically constrained calibration data sets and its application to glacial Atlantic and Pacific Oceans. Quat. Sci. Rev. 24, 951–998.

Laberg, J.S., Eilertsen, R.S., Salomonsen, G.R., 2018. Deglacial dynamics of the Vestfjorden – Trænadjupet palaeo-ice stream, northern Norway. Boreas 47, 225–237.

Laberg, J.S., Vorren, T.O., 1996. The glacier-fed fan at the mouth of Storfjorden trough, western Barents Sea: a comparative study. Geol. Rundsch. 85, 338–349.

Landvik, J.Y., Bondevik, S., Elverhøi, A., Fjeldskaar, W., Mangerud, J., Salvigsen, O., Siegert, M.J., Svendsen, J.-I., Vorren, T.O., 1998. The last glacial maximum of Svalbard and the Barents sea area: ice sheet extent and configuration. Quat. Sci. Rev. 17, 43–75.

Landvik, J.Y., Ingólfsson, Ó., Mienert, J., Lehman, S.J., Solheim, A., Elverhøi, A., Ottesen, D., 2005. Rethinking Late Weichselian ice sheet dynamics in coastal NW Svalbard. Boreas 37, 7–24.

Lehman, S.J., Keigwin, L.D., 1992. Sudden changes in North Atlantic circulation during the last deglaciation. Nature 356, 757–762.

Locarnini, R.A., Mishonov, A.V., Antonov, J.I., Boyer, T.P., Garcia, H.E., Baranova, O.K., Zweng, M.M., Johnson, D.R., 2010. World Ocean Atlas 2009, vol. 1: temperature. In: Levitus, S. (Ed.), NOAA Atlas NESDIS 68. U.S. Government Printing Office, Washington, D.C., pp. 1–184

Loeng, H., 1991. Features of the physical oceanographic conditions of the Barents Sea. Pol. Res. 10, 5–18.

Lowry, D.P., Colledge, N.R., Bertler, N.A.N., Jones, R.S., McKay, R., Stutz, J., 2020. Geologic controls on ice sheet sensitivity to deglacial climate forcing in the Ross Embayment, Antarctica. Quat. Sci. Adv. 1, 100002.

Lubinski, D.J., Polyak, L., Forman, S.L., 2001. Freshwater and Atlantic water inflows to the deep northern Barents and Kara seas since ca 13 ^{14}C ka: foraminifera and stable isotopes. Quat. Sci. Rev. 20, 1851–1879.

Luckman, A., Murray, T., de Lange, R., Hanna, E., 2006. Rapid and synchronous ice-dynamic changes in East Greenland. Geophys. Res. Lett. 33, L03503. https://doi.org/10.1029/2005GL025428.

Marcott, S.A., Clark, P.U., Padman, L., Klinkhammer, G.P., Springer, S.R., Liu, Z., Otto-Bliesner, B.L., Carlson, A.E., Ungerer, A., Padman, J., He, F., Cheng, J., Schmittner, A., 2011. Ice-shelf collapse from subsurface warming as a trigger for Heinrich events. Proc. Nat. Acad. Sci. USA 108 (13), 415–13,419.

Michel, E., Vivier, F., Party, Shipboard, 2016. 'STEP' (Storfjorden Polynya multidisciplinary study) on board Research vessel l'Atalante, Tromsø, 10 July 2016 – Tromsø, 21 July, 2016. http://ilsremontentletemps.inflexion.info/?q=node/10, 1-42.

Mouginot, J., Rignot, E., Scheugl, B., Fenty, I., Khazendar, A., Morlighem, M., Buzzi, A., Paden, J., 2015. Fast retreat of Zachariæ Isstrøm, northeast Greenland. Science 350, 1357–1361.

Murray, T., Scharrer, K., James, T.D., Rye, S.R., Hanna, E., Booth, A.D., Selmes, N., Luckman, A., Hughes, A.L.C., Cook, S., Huybrechts, P., 2010. Ocean regulation hypothesis for glacier dynamics in southeast Greenland and implications for ice sheet mass changes. J. Geophys. Res. 115 https://doi.org/10.1029/2009JF001522.

Nielsen, T., Rasmussen, T.L., 2018. Reconstruction of ice sheet retreat after the last glacial maximum in Storfjorden, southern Svalbard. Mar. Geol. 402, 228–242.

Nørgaard-Pedersen, N., Spielhagen, R.F., Erlenkeuser, H., Grootes, P.M., Heinemeier, J., Knies, J., 2003. Arctic Ocean during the Last Glacial Maximum: Atlantic and polar domains of surface water mass distribution and ice cover. Paleoceanography 18. https://doi.org/10.1029/2003PA000781.

Ó Cofaigh, C., Weilbach, K., Lloyd, J.M., Benetti, S., Callard, S.L., Purcell, C., Chiverrell, R.C., Dunlop, P., Saher, M., Livingstone, S.J., van Landeghem, K.J.J., Moreton, S.G., Clark, C.D., Fabel, D., 2019. Early deglaciation of the British-Irish Ice Sheet on the Atlantic shelf northwest of Ireland driven by glacioisostatic depression and high relative sea level. Quat. Sci. Rev. 208, 76–96.

Park, J.W., Gourmelen, N., Shepherd, A., Kim, S.W., Vaughan, D.G., Wingham, D.J., 2013. Sustained retreat of the pine Island Glacier. Geophys. Res. Lett. 40, 2137–2142.

Pedrosa, M.T., Camerlenghi, A., de Mol, B., Urgeles, R., Rebesco, M., Lucchi, R.G., Party, Shipboard, 2011. Seabed morphology and shallow sedimentary structure of the Storfjorden and Kveithola trough-mouth fans (north west Barents sea). Mar. Geol. 286, 65–81.

Petrini, M., Colleoni, F., Kirchner, N., Hughes, A.L.C., Camerlenghi, A., Rebesco, M., Lucchi, R.G., Forte, E., Colucci, R.R., Noormets, R., Mangerud, J., 2020. Simulated last deglaciation of the Barents Sea Ice Sjeet primarily driven by oceanic conditions. Quat. Sci. Rev. 238 https://doi.org/10.1016/j.quascirev.2020.106314.

Rasmussen, T.L., Thomsen, E., van Weering, T.C.E., Labeyrie, L., 1996. Rapid changes in surface and deep water conditions at the Faeroe Margin during the last 58,000 years. Paleoceanography 11, 757–771.

Rasmusssen, S.O., Bigler, M., Blockley, S.P., Blunier, T., Buchardt, S.L., Clausen, H.B., Cvijanovic, I., Dahl-Jensen, D., Johnsen, S.J., Fischer, H., Gkinis, V., Guillevic, M., Hoek, W.Z., Lowe, J.J., Pedro, J.B., Popp, T., Seierstad, I.K., Steffensen, J.P., Svensson, A.M., Vallelonga, P., Vinther, B.M., Walker, M.J.C., Wheatley, J.J., Winstrup, M., 2014. A stratigraphic framework for abrupt climatic changes during the Last Glacial period based on three synchronized Greenland ice-core records: refining and extending the INTIMATE event stratigraphy. Quat. Sci. Rev. 106, 14–28.

Rasmussen, T.L., Thomsen, E., 2004. The role of the North Atlantic Drift in the millennial timescale glacial climate fluctuations. Palaeogeogr. Palaeoclimatol. Palaeoecol. 210, 101–116.

Rasmussen, T.L., Thomsen, E., 2014. Brine formation in relation to climate changes and ice retreat during the last 15,000 years in Storfjorden, Svalbard, 76–78°N. Paleoceanography 29, 911–929.

Rasmussen, T.L., Thomsen, E., 2015. Paleoceanographic development in Storfjorden, Svalbard, during the deglaciation and Holocene: evidence from benthic foraminiferal records. Boreas 44, 24–44.

Rasmussen, T.L., Thomsen, E., Skirbekk, K., Ślubowska-Woldengen, M., Klitgaard Kristensen, D., Koç, N., 2014. Spatial and temporal distribution of Holocene temperature maxima in the northern Nordic seas: interplay of Atlantic-, Arctic- and polar water masses. Quat. Sci. Rev. 92, 280–291.

Rasmussen, T.L., Thomsen, E., Ślubowska, M.A., Jessen, S., Solheim, A., Koç, N., 2007. Paleoceanographic evolution of the SW Svalbard margin (76°N) since 20,000 ^{14}C yr BP. Quat. Res. 67, 100–114.

Reimer, P.J., Edouard, B., Bayliss, A., Beck, J.W., Blackwell, P.G., Ramsey, C.B., Buck, C.E., Cheng, H., Edwards, R.L., Friedrich, M., Grootes, P.M., Guilderson, T.P., Haflidason, H., Hajdas, I., Hatté, C., Heaton, T.J., Hoffmann, D.L., Hogg, A.G., Hughen, K.A., Kaiser, K.F., Kromer, B., Manning, S.W., Nju, M., Reimer, R.W., Richards, D.A., Scott, E.M., Southon, J.R., Staff, R.A., Turney, C.S.M., van der Plicht, J., 2013. INTCAL13 and Marine13 radiocarbon age calibration curves 0–50,000 years cal BP. Radiocarbon 55, 1869–1886.

Rignot, E., Jacobs, S., Mouginot, J., Scheuchl, B., 2013. Ice-shelf melting around Antarctica. Science 341, 266–270.

Rignot, E., Mouginot, J., Morlighem, M., Seroussi, H., Scheuchl, B., 2014. Widespread, rapid grounding line retreat of pine Island, Thwaites, Smith and Kohler glaciers, west Antarctica, from 1992–2011. Geophys. Res. Lett. 41, 3502–3509.

Rignot, E., Mouginot, J., Scheuchl, B., van den Broeke, M., van Wessem, M.J., Morlighem, M., 2019. Four decades of Antarctic ice sheet mass balance from 1979–2017. Proc. Nat. Acad. Sci. USA 116, 1095–1103.

Rintoul, S.R., Silvano, A., Pena-Molino, B., van Wijk, E., Rosenberg, M., Greenbaum, J.S., Blankenship, D.D., 2016. Ocean heat drives rapid basal melt of the Totten Ice Shelf. Sci. Adv. 2, e1601610.

Ruddiman, W.F., 1997. Late Quaternary deposition of ice-rafted sand in the subpolar North Atlantic (lat 40° to 65°N). Geol. Soc. Am. Bull. 88, 1813–1827.

Scambos, T.A., Bohlander, J.A., Shuman, C.A., Skvarca, P., 2004. Glacier acceleration and thinning after ice shelf collapse in the Larsen B embayment, Antarctica. Geophys. Res. Lett. 31, L18402. https://doi.org/10.1029/2004GL020670.

Scheuchl, B., Mouginot, J., Rignot, E., Morlighem, M., Khazendar, A., 2016. Grounding line retreat of Pope, Smith, and Kohler glaciers, west Antarctica, measured with Sentinel-1a radar interferometry data. Geophys. Res. Lett. 43, 8572–8579.

Scourse, J.D., Haapaniemi, A.I., Colmenero-Hidalgo, E., Peck, V.L., Hall, I.R., Austin, W.E.N., Knutz, P.C., Zahn, R., 2009. Growth, dynamics and deglaciation of the last British-Irish ice sheet: the deep-sea ice-rafted detritus record. Quat. Sci. Rev. 28, 3066–3084.

Sejrup, H.P., Birks, H.J.B., Klitgaard Kristensen, D., Madsen, H., 2004. Benthonic foraminiferal distributions and quantitative transfer functions for the northwest European continental margin. Mar. Micropaleontol. 53, 197–226.

Shackleton, C.S., Winsborrow, M.C.M., Andreassen, K., Lucchi, R.G., Bjarnadottir, L.R., 2020. Ice-margin retreat and grounding-zone dynamics during initial deglaciation of the Storfjordrenna Ice Stream, western Barents Sea. Boreas 49, 38–51.

Ślubowska, M.A., Koç, N., Rasmussen, T.L., Klitgaard-Kristensen, D., 2005. Changes in the flow of Atlantic water into the Arctic Ocean since the last deglaciation: evidence from the northern Svalbard continental margin, 80°N. Paleoceanography 20, PA4014. https://doi.org/10.1029/2005PA001141.

Ślubowska-Woldengen, M., Rasmussen, T.L., Koç, N., Klitgaard-Kristensen, D., Nilsen, F., Solheim, A., 2007. Advection of Atlantic Water to the western and northern Svalbard shelf since 17,500 cal yr BP. Quat. Sci. Rev. 26, 463–478.

Small, D., Smedley, R.K., Chiverell, R.C., Scourse, J.D., Ó Cofaigh, C., Duller, G.A.T., McCarron, S., Burke, M.J., Evans, D.J.A., Fabel, D., Gheorghiu, D.M., Thomas, G.S.P., Xu, S., Clark, C.D., 2018. Trough geometry was a greater influence than climate-ocean forcing in regulating retreat of the marine-based Irish Ice Stream. Geol. Soc. Am. Bull. 130, 1981–1999.

Stanford, J.D., Rohling, E.J., Bacon, S., Roberts, A.P., Grousset, F.E., Bolshaw, M., 2011. A new concept for the paleoceanographic evolution of Heinrich event 1 in the North Atlantic. Quat. Sci. Rev. 30, 1047–1066.

Steffensen, J.P., Andersen, K.K., Bigler, M., Clausen, H.B., Dahl-Jensen, D., Fischer, H., Goto-Azuma, K., Hansson, M., Johnsen, S.J., Jouzel, J., Masson-Delmotte, V., Popp, T., Rasmussen, S.O., Röthlisberger, R., Ruth, U., Stauffer, B., Siggaard-Andersen, M.-L., Sveinbjörnsdottir, A.E., Svensson, A., White, J.W.C., 2008. High-resolution Greenland ice core data show abrupt climate change happens in few years. Science 321, 680–684.

Stokes, C.R., Corner, G.D., Winsborrow, M.C.M., Husum, K., Andreassen, K., 2014. Asynchronous response of marine-terminating outlet glaciers during deglaciation of the Fennoscandian Ice Sheet. Geology 42, 455–458.

Svendsen, J.I., Elverhøi, A., Mangerud, J., 1996. The retreat of the Barents sea ice sheet on the western Svalbard margin. Boreas 25, 244–256.

Tian, S.Y., Yasuhara, M., Hong, Y., Huang, H.-H.M., Iwatani, H., Chiu, W.-T.R., Mamo, B., Okahashi, H., Rasmussen, T.L., 2020. Deglacial–holocene Svalbard paleoceanography and evidence of melt water pulse 1B. Quat. Sci. Rev. 233 https://doi.org/10.1016/j.quascirev.2020.106237.

Voelker, A.H.L., Haflidason, H., 2015. Refining the Icelandic tephrachronology of the last glacial period – the deep-sea core PS2644 record from the southern Greenland Sea. Global Planet. Change 131, 35–62.

Voelker, A.H.L., Sarnthein, M., Grootes, P.M., Erlenkeuser, H., Laj, C., Mazaud, A., Nadeau, M.-J., 1998. Correlation of marine ^{14}C ages from the Nordic seas with the GISP2 isotope record: implications for ^{14}C calibration beyond 25 ka BP. Radiocarbon 40, 517–531.

Vorren, T.O., Plassen, L., 2002. Deglaciation and palaeoclimate of the Andfjord-Vågsfjord area, north Norway. Boreas 31, 97–125.

Waelbroeck, C., Duplessy, J.-C., Michel, E., Laberyrie, L., Paillard, D., Duprat, J., 2001. The timing of the last deglaciation in North Atlantic climate records. Nature 412, 724–727.

Waelbroeck, C., et al., 2019. Consistently dated Atlantic sediment cores over the last 40 thousand years. Sci. Data 6. https://doi.org/10.1038/s41597-019-0173-8.